iScience

CellPress
OPEN ACCESS

Article

Timed exercise stabilizes behavioral rhythms but not molecular programs in the brain's suprachiasmatic clock

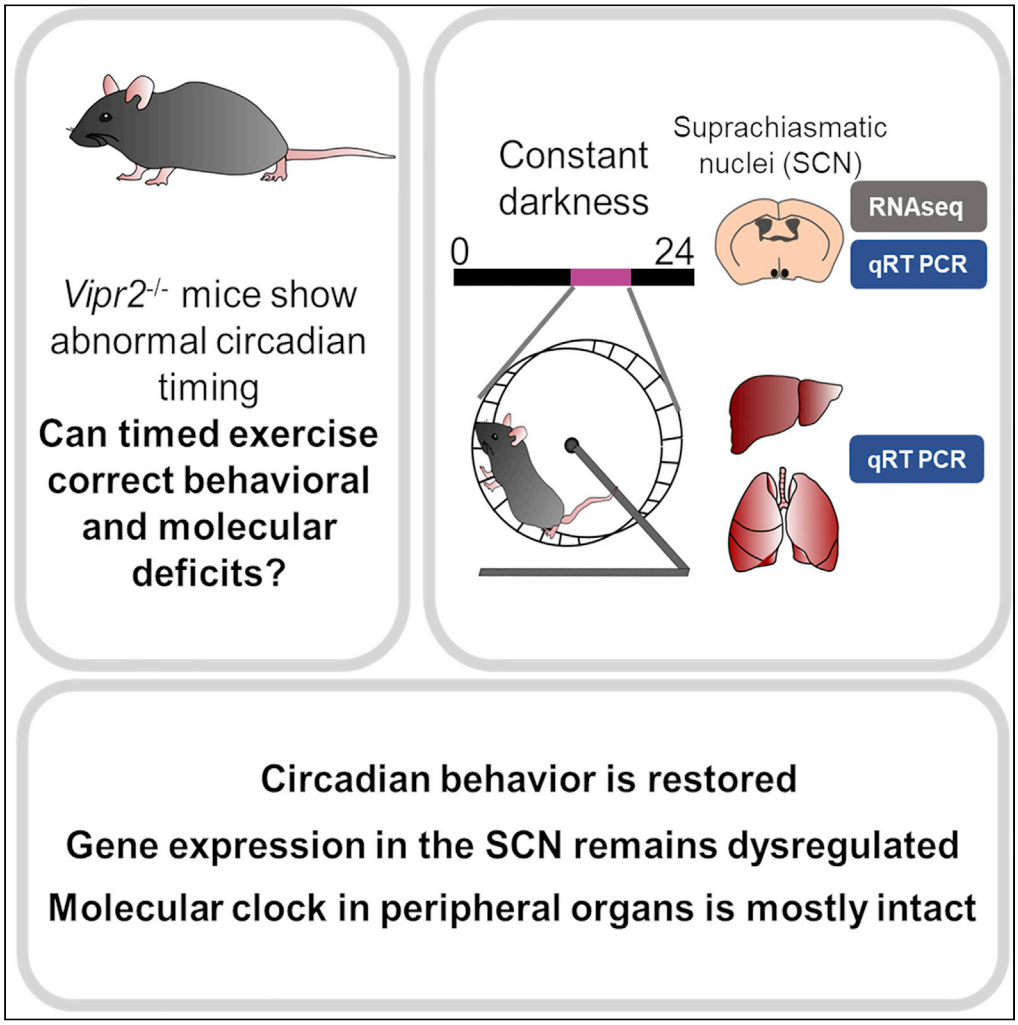

Timna Hitrec, Cheryl Petit, Emily Cryer, ..., Jean-Michel Fustin, Alun T.L. Hughes, Hugh D. Piggins

a.t.hughes@ljmu.ac.uk (A.T.L.H.)
hugh.piggins@bristol.ac.uk (H.D.P.)

Highlights

Timed exercise promotes stable behavioral rhythms in $VPAC_2$ deficient mice

Loss of $VPAC_2$ dysregulates the suprachiasmatic (SCN) transcriptome

Timed exercise does not restore the SCN transcriptome in $VPAC_2$ deficient mice

Behavioral effects of timed exercise require a functional molecular clock

Hitrec et al., iScience 26, 106002
February 17, 2023
https://doi.org/10.1016/j.isci.2023.106002

iScience

CellPress
OPEN ACCESS

Article

Timed exercise stabilizes behavioral rhythms but not molecular programs in the brain's suprachiasmatic clock

Timna Hitrec,[1] Cheryl Petit,[2] Emily Cryer,[3] Charlotte Muir,[1] Natalie Tal,[2] Jean-Michel Fustin,[2] Alun T.L. Hughes,[2,4,*] and Hugh D. Piggins[1,2,5,*]

SUMMARY

Timed daily access to a running-wheel (scheduled voluntary exercise; SVE) synchronizes rodent circadian rhythms and promotes stable, 24h rhythms in animals with genetically targeted impairment of neuropeptide signaling (*Vipr2*$^{-/-}$ mice). Here we used RNA-seq and/or qRT-PCR to assess how this neuropeptide signaling impairment as well as SVE shapes molecular programs in the brain clock (suprachiasmatic nuclei; SCN) and peripheral tissues (liver and lung). Compared to *Vipr2*$^{+/+}$ animals, the SCN transcriptome of *Vipr2*$^{-/-}$ mice showed extensive dysregulation which included core clock components, transcription factors, and neurochemicals. Furthermore, although SVE stabilized behavioral rhythms in these animals, the SCN transcriptome remained dysregulated. The molecular programs in the lung and liver of *Vipr2*$^{-/-}$ mice were partially intact, although their response to SVE differed to that of these peripheral tissues in the *Vipr2*$^{+/+}$ mice. These findings highlight that SVE can correct behavioral abnormalities in circadian rhythms without causing large scale alterations to the SCN transcriptome.

INTRODUCTION

Circadian or intrinsic 24h rhythms in mammalian physiology and behavior are generated by the brain's suprachiasmatic nuclei (SCN).[1] The SCN is synchronized or entrained to the external world by zeitgebers including environmental light (photic information)[2] and feedback from arousal-promoting or non-photic cues, such as mealtimes and social interactions.[3–5] Photic and non-photic signals are relayed to the SCN by different neural pathways using different neurotransmitters and thereby represent very different channels and modes of information.[6]

Cells of the SCN express daily rhythms in clock genes such as *Per1-2*, *Clock*, and *Arntl*[7] and this molecular circadian clockwork enables them to function as autonomous cellular oscillators. The same molecular machinery is also active in peripheral tissues, for instance allowing cells in the lungs and liver to act as peripheral oscillators.[8,9] The neuropeptide vasoactive intestinal polypeptide (VIP) and its cognate receptor $VPAC_2$, are synthesized by SCN cells and this intercellular VIP-$VPAC_2$ signaling is necessary for clock cells in the SCN to synchronize their timekeeping.[10,11] In mice with genetically targeted impairment of $VPAC_2$ receptor expression (*Vipr2*$^{-/-}$ mice), SCN clock cells are poorly coordinated and these animals exhibit abnormal rhythms in behavior or are completely arrhythmic.[12,13] Furthermore, processing of photic input is dysfunctional in the *Vipr2*$^{-/-}$ SCN and these animals show aberrant entrainment to the light-dark cycle.[13]

Regular physical exercise promotes good health[14,15] and in both natural and laboratory settings, rodents voluntarily exercise vigorously in running wheels.[16–18] Exercising at the same time of day through timed daily access to a running wheel, or scheduled voluntary exercise (SVE), is an effective non-photic cue for rodents.[19,20] Indeed, SVE can restore some SCN function and promote 24h behavioral rhythms in *Vipr2*$^{-/-}$ mice.[21,22] The SCN of *Vipr2*$^{-/-}$ mice shows marked impairment in clock gene expression[12,23] and longitudinal *ex vivo* assessment of *Vipr2*$^{-/-}$ SCN cells expressing *Per1* indicates that SVE increases the number and synchrony of such cells.[21] However, the extent to which SVE corrects deficits in molecular clock gene expression as well as that of the wider molecular programs in the *Vipr2*$^{-/-}$ SCN remains unclear.

[1]School of Physiology, Pharmacology, and Neuroscience, Faculty of Life Sciences, University of Bristol, Bristol BS8 1TD, UK

[2]School of Medical Sciences, Faculty of Biology, Medicine, and Health, University of Manchester, Manchester M13 9PT, UK

[3]School of Biological Sciences, Faculty of Life Sciences, University of Bristol, Bristol BS8 1TQ, UK

[4]School of Biological and Environmental Sciences, Faculty of Science, Liverpool John Moores University, Liverpool L3 3AF, UK

[5]Lead contact

*Correspondence: a.t.hughes@ljmu.ac.uk (A.T.L.H.), hugh.piggins@bristol.ac.uk (H.D.P.)

https://doi.org/10.1016/j.isci.2023.106002

Both microarray and next generation sequencing approaches have been extensively used to study how light affects the SCN transcriptome,[24–26] but very little is known regarding the equivalent effects of non-photic cues. In this investigation, we address this important gap in our knowledge by using RNA-seq and/or qRT-PCR to assess molecular programs in the SCN, lungs and liver and determine how these are altered by loss of the $VPAC_2$ receptor and how they are influenced by timed exercise. In *Vipr2*$^{-/-}$ mice rhythmic when freely exercising, we find much more extensive alteration in the SCN transcriptome than previously reported, whereas gene expression in the lung and liver of these animals is mostly intact. In addition to clock genes (*Per2*, *Nr1d1*), factors implicated in regulating the SCN clock (*Ncor1 C1ql3 Gpr176)*, the transcription of hypothalamic neuropeptides (*Creb3l1*), SCN neuropeptides (*Penk*, *Avp*, *Prok2, Sst*, and *Vip*), and a key potassium channel subunit (*Kcnc2*) are dysregulated in the *Vipr2*$^{-/-}$ SCN. Further, several addiction pathways are upregulated in the *Vipr2*$^{-/-}$ SCN, suggesting that these mice are more responsive to the rewarding properties of exercising in a running wheel.[27] For *Vipr2*$^{+/+}$ mice, exposure to SVE caused small changes in the period of behavioral activity and altered molecular clock (*Arntl*) and neuropeptide (*Avp, Prok2*) expression in the SCN. This suggests that in the neurochemically intact SCN, timed exercise evokes changes through reducing neurochemical signaling. By contrast, SVE profoundly re-organizes the daily profile of ingestive and locomotor behavior of *Vipr2*$^{-/-}$ animals to more closely resemble that of *Vipr2*$^{+/+}$ mice. Surprisingly this is not accompanied by widespread restoration of gene expression in the SCN, but notably, pathways associated with neurodegeneration are downregulated by timed exercise in the *Vipr2*$^{-/-}$ SCN. This suggests that SVE is neuroprotective in these animals. Mice lacking a functional molecular clock respond to timed exercise, but unlike *Vipr2*$^{-/-}$ animals, they do not sustain 24h behavioral rhythms when the exercise regimen is terminated. Collectively, these findings reveal a grossly dysregulated SCN transcriptome in behaviorally rhythmic *Vipr2*$^{-/-}$ mice which surprisingly remains uncorrected despite the behavior modifying actions by timed exercise. Therefore, either a minimally functional molecular SCN clock can orchestrate behavioral rhythms and/or SVE recruits extra-SCN oscillators to circumvent the SCN and stabilize behavioral rhythms.

RESULTS

Vipr2$^{-/-}$ mice readily align their circadian rhythm when subjected to a scheduled exercise protocol

Patterns of daily food intake can influence gene expression in the liver and the hypothalamus.[28–30] Because it is unclear how loss of the $VPAC_2$ receptor affects the relationship between daily rhythms in ingestive behavior and locomotor activity, we determined the precise circadian patterns of feeding and drinking behavior in C57BL/6J (*Vipr2*$^{+/+}$) and *Vipr2*$^{-/-}$ mice exhibiting rhythms in voluntary non-scheduled exercise (nSVE) wheel-running in constant dark (see Figure 1 for protocol, Figures 2A and 2B). *Vipr2*$^{-/-}$ animals had an accelerated period ~22.9h (22.94 $\pm$ 0.29h; mean $\pm$ SEM) in wheel-running that was more variable and significantly shorter than that of *Vipr2*$^{+/+}$ mice (23.61 $\pm$ 0.02h). Both genotypes ran in the running-wheels for similar distances over the circadian cycle (~4–6 km; $p>0.05$), but over the first half of the night (CT12-18), *Vipr2*$^{+/+}$ mice exercised more intensely (up to ~932 vs ~533 cm/min) and ran farther than *Vipr2*$^{-/-}$ animals (~2.4 versus ~1.9 km respectively; $p<0.01$; Figure 2C). Feeding and drinking also differed between the genotypes, with *Vipr2*$^{+/+}$ mice consuming more food and water over the circadian cycle than *Vipr2*$^{-/-}$ mice (both $p<0.05$) and drinking more water than *Vipr2*$^{-/-}$ mice across the first half of the night (~1.9 vs ~0.3 mL; $p<0.01$). The contour in ingestive behaviors in *Vipr2*$^{+/+}$ animals was delayed with respect to wheel-running and they achieved 50% of the nightly maxima ~1.1h (food) and ~4.3h (water) after that of wheel-running. This delayed profile was much less noticeable in *Vipr2*$^{-/-}$ animals and they reached 50% of the nightly maxima within ~0.7h of the increase in wheel-running. Thus, loss of the $VPAC_2$ receptor influences the circadian pattern and phase relationships between wheel-running and ingestive behaviors.

In the scheduled voluntary exercise (SVE) experiment the running-wheel can be exercised in for a set 6h per 24h, with the onset of the drinking rhythm (CT12) used to estimate circadian phase. *Vipr2*$^{-/-}$ mice responded rapidly to timed wheel-availability (Figure 2A) and fully entrained within 14 days such that their CT12 was aligned to the start time of wheel availability (ZT12). In contrast, *Vipr2*$^{+/+}$ animals adjusted much more slowly and aligned to the opportunity to exercise at a different phase than *Vipr2*$^{-/-}$ mice. *Vipr2*$^{+/+}$ animals achieved a 24h drinking rhythm after ~35–40 days with their CT12 ~8h in advance of wheel availability and consequently, their CT20 corresponds with ZT12 (see Figure 1). Neither genotype ran as far during the 6h of SVE as they had over the circadian cycle under nSVE conditions, but *Vipr2*$^{-/-}$ mice ran more intensely and farther during SVE CT12-18 than they did over this 6h phase in the nSVE condition (~2.9 vs 1.9 km; $p<0.05$) to more closely resemble the wheel-running profile seen in *Vipr2*$^{+/+}$ mice over

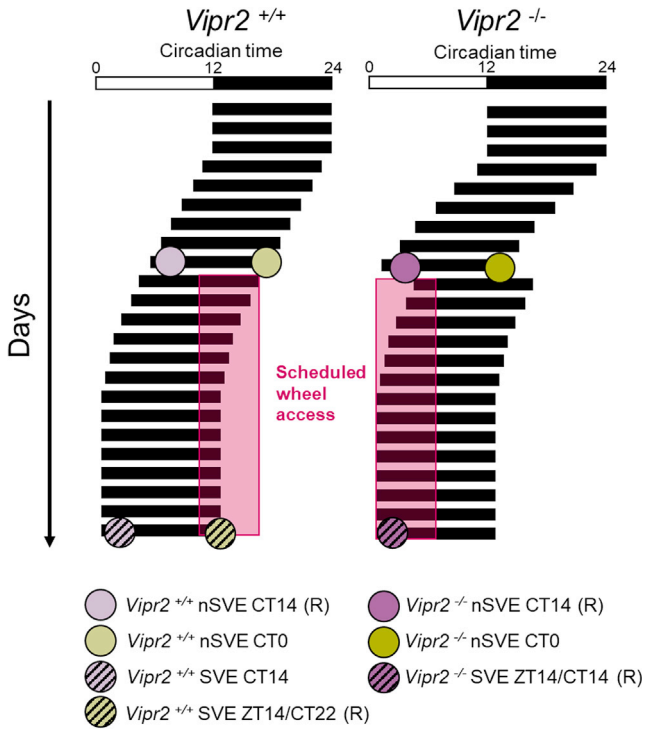

Figure 1. Graphical depiction of the experimental design of the scheduled voluntary exercise (SVE) and tissue sampling protocols

Horizontal black bars represent drinking activity across the circadian cycle for exemplar mice from each genotype. Following entrainment to the Light-Dark cycle, mice were transferred to constant dark and left to free-run in the non-Scheduled exercise study (nSVE), where the *Vipr2*$^{+/+}$ mouse has approx. 23.3h rhythm and a rhythmic *Vipr2*$^{-/-}$ mouse an approx. 22.5h rhythm. Non-SVE mice of both genotypes were culled at CT14 (pale purple in *Vipr2*$^{+/+}$ and purple in *Vipr2*$^{-/-}$) and CT0 (pale green in *Vipr2*$^{+/+}$ and green in *Vipr2*$^{-/-}$). During the SVE regimen, the running-wheel can be rotated by the animal for a set 6 h/day (pink box). Under SVE, the *Vipr2*$^{+/+}$ mouse initiates drinking approx. eight hours in advance of wheel availability, whereas the *Vipr2*$^{-/-}$ mouse quickly aligns onset of drinking behavior with the onset of wheel availability. Under SVE, mice were culled 2 h after wheel availability (ZT14; striped pale green in *Vipr2*$^{+/+}$ and striped purple in *Vipr2*$^{-/-}$). Because *Vipr2*$^{+/+}$ mice do not align the onset of drinking with the onset of wheel availability, additional *Vipr2*$^{+/+}$ mice were culled at CT14 (striped pale purple). Tissue for all conditions was sampled for RT-qPCR, whereas tissue used for RNA-seq was restricted to four groups, marked with (R).

CT12-18 of the nSVE condition. *Vipr2*$^{+/+}$ animals consumed more food and water over the circadian cycle than *Vipr2*$^{-/-}$ mice (both $p<0.05$). However, animals lacking the $VPAC_2$ receptor increased food and water consumption (Figures 2B and 2C) during the 6h of timed exercise (relative to the CT12-18 of the nSVE condition) such that there were no genotype differences in ingestive parameters over the 6h of SVE. Notably, the profiles of locomotor and ingestive behavior of *Vipr2*$^{-/-}$ mice under SVE approximated that of *Vipr2*$^{+/+}$ animals under the nSVE condition. Therefore, consistent with the increased intensity in wheel-running, timed-exercise also elevates the intensity of food and water consumption in *Vipr2*$^{-/-}$ mice to resemble that of *Vipr2*$^{+/+}$ animals. Consequently, differences in the molecular programs in the liver, lung, and SCN arising from loss of the $VPAC_2$ receptor under the nSVE condition should be corrected through entrainment of *Vipr2*$^{-/-}$ mice to scheduled voluntary exercise.

Assessing loss of $VPAC_2$ receptor expression and timed exercise on the SCN transcriptome by RNA-seq

To comprehensively define the molecular correlates of the loss of $VPAC_2$ receptors on the mouse SCN and to explore how the SCN transcriptome can be modified by SVE, we performed RNA-seq on laser-captured microdissected SCN in four experimental groups: *Vipr2*$^{+/+}$ nSVE CT14, *Vipr2*$^{-/-}$ nSVE CT14, *Vipr2*$^{+/+}$ SVE ZT14/CT22 and *Vipr2*$^{-/-}$ SVE ZT14/CT14 (subsequently abbreviated as *Vipr2*$^{+/+}$ nSVE, *Vipr2*$^{-/-}$ nSVE, *Vipr2*$^{+/+}$ SVE, *Vipr2*$^{-/-}$ SVE). As illustrated in Figures 1 and 2, the CT14 timepoint in the nSVE condition is comparable between genotypes, as it controls for both circadian time as well as number of hours

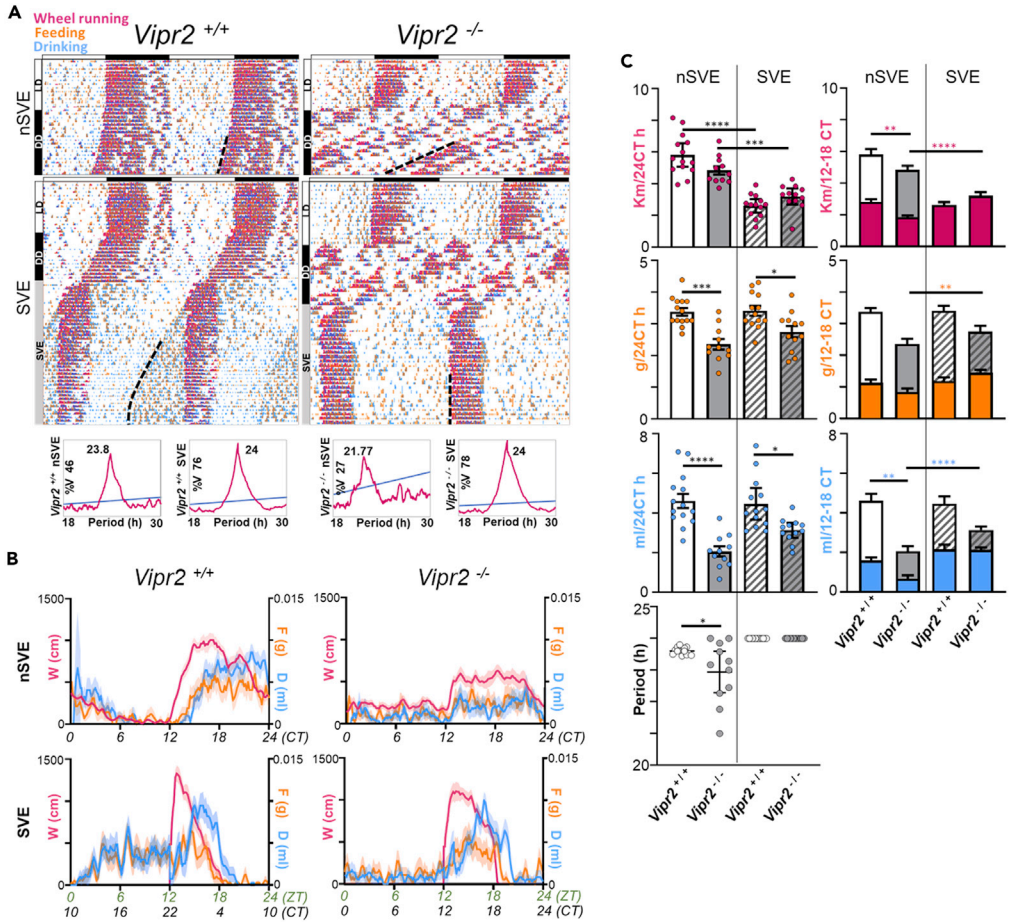

Figure 2. Scheduled voluntary exercise re-organizes murine behavioral activity rhythms

(A) Double plotted actograms of wheel running (pink), feeding (orange) and drinking (blue) rhythms from individual *Vipr2*$^{+/+}$ and *Vipr2*$^{-/-}$ mice recorded for the non-Scheduled voluntary exercise (nSVE) and scheduled voluntary exercise (SVE) studies. Following two weeks under the light-dark condition (LD), the lights were left off and the mice maintained in constant dark (DD) for the remainder of the experiment. For the nSVE study, animals free-ran in DD for 3–4 weeks; for mice allocated to the SVE experiment, they free-ran for 2 weeks and then the timed exercise regimen (voluntary wheel-running for 6h/24h) was initiated. The periodograms below the actograms indicate the dominant frequency in wheel-running (averaged over the final 10 days of recording for nSVE or 7 days for SVE (Horizontal black/white bar = LD cycle in the first two weeks, % V = percentage of variance).

(B) Average profile of wheel running (W, pink), feeding (F, orange) and drinking (D, blue) in either circadian time (CT; nSVE) or zeitgeber time (ZT; SVE). Because the free-running period varied from *Vipr2*$^{-/-}$ to *Vipr2*$^{+/+}$ mice, CT hours were adjusted appropriately. Parameters for the profiles are based on measures taken over the final 10 days of the nSVE experiment or final 7 days of the SVE experiment. Profile lines plot the average value ±SEM, and were calculated on 10-min sample bins, and then smoothed with a 30-min moving average. The circadian day-night profile of *Vipr2*$^{-/-}$ mice is damped compared to *Vipr2*$^{+/+}$ animals. Under SVE conditions, *Vipr2*$^{-/-}$ animals readily synchronize the beginning of their circadian night (CT12) to wheel availability (ZT12), whereas *Vipr2*$^{+/+}$ animals initiate their circadian night approx. 8h in advance of ZT12.

(C) *Left column:* Average cumulative value of wheel-running (pink), feeding (orange) and drinking (blue) in 24 circadian hours for *Vipr2*$^{+/+}$ (white) and *Vipr2*$^{-/-}$ (gray), in nSVE (solid) and SVE (striped) mice (mean ±95% C.I., calculated for 10 days in nSVE, 7 days for SVE). The bottom panel plots the period of running wheel activity of individual animals in the four experimental groups. *Right column:* filled histograms represent the average amount of wheel-running/feeding/drinking during the first 6 h from CT12 or ZT12 (coinciding with wheel availability), superimposed on the total daily amount. Compared to the nSVE condition, *Vipr2*$^{-/-}$ mice in the SVE condition significantly increase their drinking and feeding behavior during ZT 12–18. (mean ±95% C.I., calculated for 10 days in nSVE, 7 days for SVE, p value <0.05 = *, <0.01 = **, <0.005 = ***, <0.001 = ****, ANOVA and *a priori* post-hoc unpaired *t* test, *Vipr2*$^{+/+}$ nSVE n=14, *Vipr2*$^{-/-}$nSVE n=11, *Vipr2*$^{+/+}$ SVE n=13, *Vipr2*$^{-/-}$ SVE n=12).

exercising in a running wheel. This corresponds to a circadian phase at which clock gene expression in the SCN is known to be different between the two genotypes of mice.[12] In SVE conditions, *Vipr2*$^{-/-}$ mice readily align their drinking activity to the wheel availability, and hence their CT14 corresponds to ZT14. This allows direct comparison between the nSVE and SVE conditions for assessing scheduled exercise related changes in the *Vipr2*$^{-/-}$ SCN transcriptome. The situation is different in *Vipr2*$^{+/+}$ mice, because in the SVE condition their onset of drinking activity precedes wheel availability by ~8 h, thereby resulting in two distinct timepoints for CT14 and ZT14/CT22. Therefore, in the SVE condition, we chose to control for the number of hours of wheel running and sampled the *Vipr2*$^{+/+}$ mice at ZT14/CT22.

We compared differentially expressed genes [(DEGs) with False Discovery Rate (FDR) < 0.05] across genotypes and exercise conditions. Principal components analysis indicated a tendency for genotype and experimental condition samples to cluster (Figure S1). The data can be accessed at GEO: GSE207992 (https://www.ncbi.nlm.nih.gov/geo/query/).

Loss of VPAC$_2$receptor dysregulates the SCN transcriptome

To examine how the loss the VPAC$_2$ receptor affects the SCN transcriptome, we compared SCN tissue from nSVE *Vipr2*$^{-/-}$ and nSVE *Vipr2*$^{+/+}$ mice sampled at CT14. We found 307 DEGs, with 158 upregulated and 149 downregulated in the *Vipr2*$^{-/-}$ SCN (Figure 3A). Notably, the four most upregulated transcripts (transmembrane proteins *Tmem254b*, *Tmem254c*, and *Glypican-3 or Gpc3*) as well as a strongly downregulated transcript, kinase insert domain receptor (*Kdr*) have no known function in SCN circadian timekeeping, though *Kdr* may have a role in circadian rhythms in peripheral tissues[31] and both *Kdr* and *Gpc3* have potential involvement in carcinoma processes.[32,33] Proenkephalin (*Penk*) whose expression defines a subpopulation of SCN neurons in the dorsal or shell subregion[34] was upregulated in the *Vipr2*$^{-/-}$ SCN. A large number of genes were downregulated in the *Vipr2*$^{-/-}$ SCN including factors known to regulate circadian rhythms in other tissues, such as nuclear co-repressor receptor 1 (*Ncor1*)[35] as well as the SCN complement 1q-like 3 protein (*C1ql3*).[36] Other prominently downregulated genes include those for neuropeptides that are key to SCN function (*Vip*)[12] and communication of circadian information both within the SCN and to the rest of the brain, arginine-vasopressin (*Avp*).[37] The VPAC$_2$ receptor is positively coupled to adenylate cyclase[38] and notably the transcription factor, cyclic AMP response element binding protein 3-like 1 (*Creb3l1*) which can regulate *Avp* transcription[39] was downregulated. Neurons of the *Vipr2*$^{-/-}$ SCN are hyperpolarized[40] and hypoactive[21,41] and an important potassium channel subunit in shaping SCN neuronal excitability (*Kcnc2*)[42] was downregulated in the *Vipr2*$^{-/-}$ SCN. In addition, molecular programs in non-neuronal SCN cells may be affected by the loss of the VPAC$_2$ receptor. For example, myelin-associated oligodendrocytic basic protein (*Mobp*)[43] was downregulated in the *Vipr2*$^{-/-}$ SCN.

These findings indicate that wide-ranging alterations in the SCN transcriptome arise as a consequence of the loss of VPAC$_2$ receptor expression. Indeed, KEGG[44] analysis indicated that the top pathways affected were all upregulated in the *Vipr2*$^{-/-}$ SCN including the terms of substance abuse ('Alcoholism', 'Amphetamine addiction', 'Cocaine addiction', 'Morphine addiction') as well as neurochemical signaling ('Serotonergic synapse', 'Dopaminergic synapse', 'Glutamatergic synapse', 'Relaxin signaling pathway', 'GABAergic synapse' etc) (Figure 3B, for extended data see Figure S2). This suggests that *Vipr2*$^{-/-}$ mice are responsive to rewarding properties of stimuli and that GABA signaling in the SCN of these animals is altered. This latter possibility is supported by observations of reduced neuronal activity and altered responses to GABAergic blockade in the *Vipr2*$^{-/-}$ SCN.[21] Gene Ontology (GO) analysis of biological process indicated a broad range of alterations including enrichment for terms such as 'regulation of protein localization', 'regulation of hormone levels', and 'intracellular signal transduction' (Figure S3). Thus, several pathways and processes are altered in the SCN through loss of the VPAC$_2$ receptor. These are presumably attributable to both weakening of the SCN molecular clock as well as changes in the timing of feedback signals arising from the altered pattern of daily food intake (Figure 2).

Circadian and exercise regulation of the SCN transcriptome

To evaluate effects of scheduled exercise and circadian time on the transcriptome of the neurochemically intact SCN, we compared SCN tissue from SVE *Vipr2*$^{+/+}$ mice sampled at ZT14/CT22 and nSVE *Vipr2*$^{+/+}$ mice sampled at CT14 (Figure 3C). Several DEGs were detected (n = 795), with 556 upregulated and 239 downregulated in the SVE condition, including core components of the molecular circadian clock (upregulated: *Nr1d1*; downregulated: *Cry1* and *Per2*) (Figure S4). Furthermore, *Rgs16*, which is known to influence SCN circadian timekeeping[45] was upregulated in the SVE condition at ZT14/CT22. In addition, expression

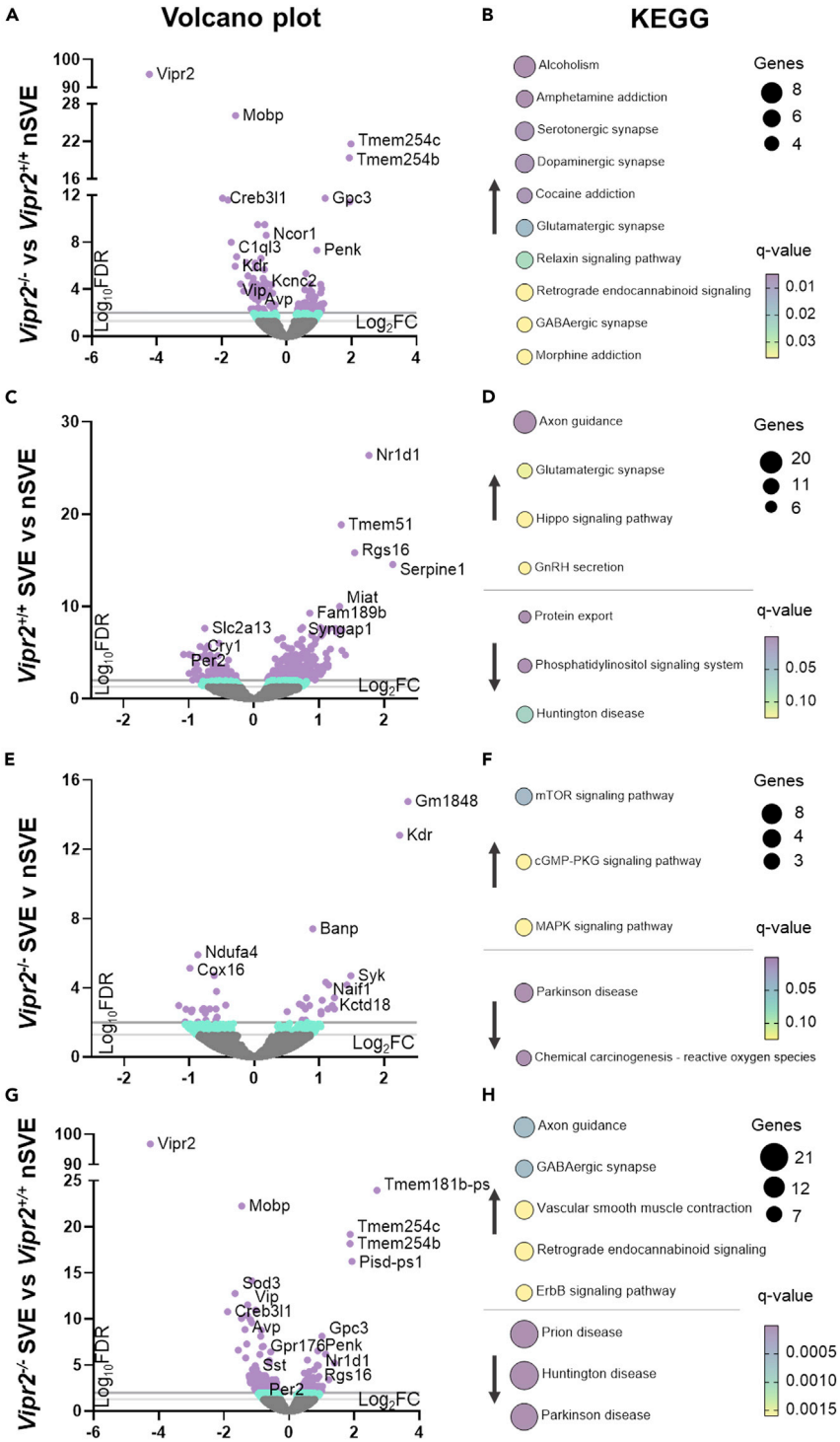

Figure 3. Genotype and exercise differential alter gene expression in the suprachiasmatic nuclei

Left: Volcano plots (A, C, E, and G) showing the differentially expressed genes in the comparisons (A) *Vipr2*$^{-/-}$ vs *Vipr2*$^{+/+}$ nSVE, (C) *Vipr2*$^{+/+}$ SVE vs nSVE, (E) *Vipr2*$^{-/-}$ SVE vs nSVE and (G) *Vipr2*$^{-/-}$ SVE vs *Vipr2*$^{+/+}$ nSVE. Genes that are not significantly differentially regulated are shown in gray, genes significantly differentially expressed, with $Log_{10}FDR$ between 0.05 and 0.01 are in turquoise, in purple genes with $Log_{10}FDR<0.01$. *Right:* The correspondingly 10 most enriched terms (B, D, F, and H) in the KEGG database for functional enrichment of genes (Kyoto Encyclopedia of Genes and Genomes). The size of the circle is a representation of the number of genes that have been annotated, whereas the color is indicative of the q-value. The arrows indicate the direction of regulation (↑ upregulated, ↓ downregulated).

of factors implicated in cancer varied, with myocardial-infarction associated transcript (*Miat*) upregulated at ZT14/CT22 in the SVE condition, whereas proton myo-inositol co-transporter (*Slc2a13*) was downregulated. The plasminogen activator inhibitor 1 (*Serpine1*) which is implicated in thrombophilia[46] was upregulated at ZT14/CT22 as was synaptic ras GTPase-activating protein 1 (*Syngap1*), which is important for synaptic development.[47] Unsurprisingly, KEGG analysis indicated that several pathways were upregulated at ZT14/CT22 of the SVE condition ('Axon guidance', 'Glutamatergic synapse', 'Hippo signaling pathway' etc), whereas others were downregulated ('Protein export', 'Phosphatidylinositol signaling system', and 'Huntington disease' etc) (Figure 3D, for extended data see Figure S2). The GO terms 'cell junction organization', 'cell-cell signaling' and 'synapse organization' were among those prominently enriched in this comparison (Figure S3). The circadian phases sampled in the SVE and nSVE conditions varied by 8h and therefore the pattern of DEGs found here is representative of known circadian changes in SCN gene expression as well as the actions of wheel-running for 2 h at the late-night phase.

Scheduled exercise does not restore the *Vipr2*$^{-/-}$ SCN molecular clock

To ascertain how the period lengthening effects of entrainment to timed-exercise affects the SCN transcriptome of *Vipr2*$^{-/-}$ animals, we compared SCN tissue from SVE and nSVE *Vipr2*$^{-/-}$ animals sampled at SVE ZT14/CT14 and nSVE CT14. We detected 223 DEGs, with 105 upregulated in the SVE animals, and 118 downregulated (Figure 3E), but surprisingly no core circadian clock genes where differentially expressed. Excluding the pseudogene (*Gm1848*), genes prominently upregulated by timed-exercise include *Kdr*, BTG3 associated nuclear protein (*Banp*), spleen non-receptor tyrosine kinase (*Syk*), Nuclear Apoptosis Inducing Factor 1 (*Naif1*) and potassium channel tetramerization domain containing 18 (*Kctd18*). These represent diverse processes potentially altered by exercise. For example, *Banp* is implicated in chromatin remodeling and neuronal differentiation,[48] whereas *Kctd18* may have involvement in the sleep disorder, restless leg syndrome.[49] Genes whose expression in the *Vipr2*$^{-/-}$ SCN was downregulated by SVE include cytochrome *c* oxidase assembly factor 16 (*Cox16*) and reduced form of nicotinamide adenine dinucleotide dehydrogenase (ubiquinone) 1α subcomplex subunit 4 (*Ndufa4*). *Ndufa4* is implicated in inflammatory responses and in particular that of mitochondrial cytochrome *c* oxidase.[50] KEGG analysis indicates that the pathways 'Parkinson disease' and 'Chemical carcinogenesis-reactive oxygen species' are among the pathways upregulated by timed exercise, whereas 'mTOR signaling pathway' (Figure 3F, for extended data see Figure S2), which is implicated in physiological responses to exercise in peripheral tissues is downregulated.[51,52] GO enrichment terms found in this comparison include 'intracellular protein transport' and 'negative regulation of catabolic process' (Figure S3). Therefore, timed exercise differentially regulates the expression of several intracellular processes including chromatin remodeling and inflammatory response, but notably, alteration of clock genes does not feature.

Feedback from behavioral and ingestive states shapes the *Vipr2*$^{-/-}$ SCN transcriptome

Under nSVE conditions, the circadian profiles of ingestive and wheel-running behaviors differs between *Vipr2*$^{+/+}$ and *Vipr2*$^{-/-}$ mice (Figures 2B and 2C) and this could contribute to the genotype-related DEGs. Therefore to compare between these genotypes at a similar CT and under conditions at which their patterns of ingestive and locomotor behavior are more equivalent (Figure 2B), we assessed SCN tissue from the SVE *Vipr2*$^{-/-}$ animals sampled at ZT14/CT14 and nSVE *Vipr2*$^{+/+}$ mice sampled at CT14 (Figure 3G). This comparison yielded 557 DEGs, with 246 upregulated and 311 downregulated in the SCN of SVE *Vipr2*$^{-/-}$ mice. Aside from the transmembrane protein genes (*Tmem181b-ps and Tmem254b,c*) and the pseudogene phosphatidylserine decarboxylase, pseudogene 1 (*Pisd-ps1*), genes prominently upregulated in *Vipr2*$^{-/-}$ mice include *Gpc3*, *Penk*, and *Rgs16* as well as the molecular clock component, *Nr1d1*. Downregulated genes in *Vipr2*$^{-/-}$ animals include *Mobp* and *Creb3l1* as well as the neuropeptides *Avp*, *Vip*, and somatostatin (*Sst*). Furthermore, the clock gene *Per2* and the orphan receptor, *Gpr176,* which influences SCN circadian timekeeping,[53] were downregulated in the SVE *Vipr2*$^{-/-}$ SCN as was superoxide dismutase 3 (*Sod3*), which protects tissues against oxidative stress[54] (Figure 3G). As a number of these differences were seen when comparing *Vipr2*$^{-/-}$ and *Vipr2*$^{+/+}$ mice in nSVE conditions (*Gpc3* and *Penk* upregulated with *Avp*, *Vip*, *Mobp*, and *Creb3l1* downregulated; Figure 3A), then this indicates that entrainment of *Vipr2*$^{-/-}$ mice to timed exercise does not restore SCN expression of these genes to *Vipr2*$^{+/+}$ like levels. Furthermore, as clock gene expression remains low in the *Vipr2*$^{-/-}$ mice, then SVE does not appear to overtly augment molecular clock gene expression in the *Vipr2*$^{-/-}$ SCN.

However, both KEGG and GO pathway analysis indicated enrichment in terms not seen in the nSVE *Vipr2*$^{-/-}$ vs nSVE *Vipr2*$^{+/+}$ comparison (Figures 3H, S2, and S3). This suggests that entrainment to timed

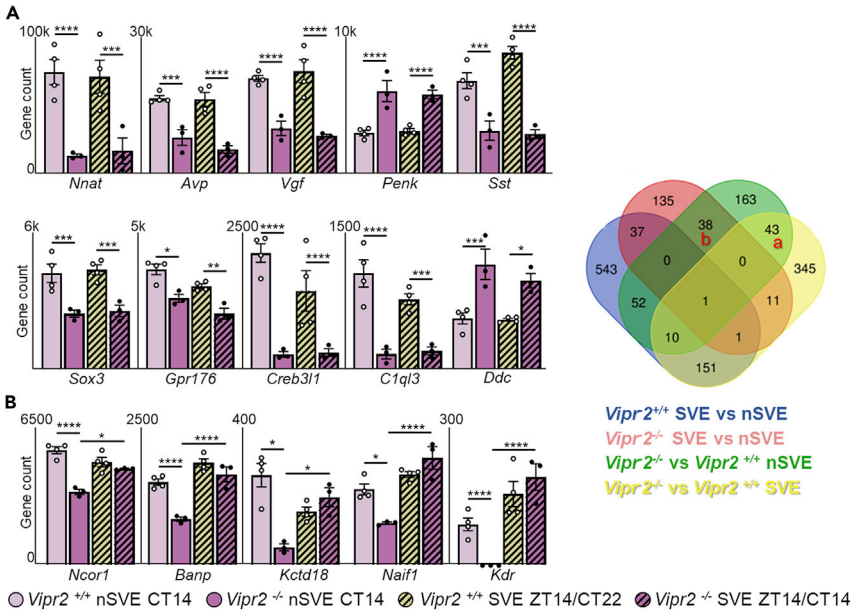

Figure 4. RNA-seq gene expression counts of a selection of genes that are differentially expressed amongst experimental groups

Genes have been grouped by significance comparisons as illustrated in the Venn diagram on the right. For example, *Nnat* is amongst the 43 genes (A) that are differentially expressed in the comparisons *Vipr2*$^{-/-}$ vs *Vipr2*$^{+/+}$ nSVE and *Vipr2*$^{-/-}$ vs *Vipr2*$^{+/+}$ SVE (intersection between the green and yellow sets), whereas the expression of *Ncor1* (B) differs between genotypes and is upregulated in the SVE condition of *Vipr2*$^{-/-}$ mice (comparisons *Vipr2*$^{-/-}$ vs *Vipr2*$^{+/+}$ nSVE and *Vipr2*$^{-/-}$ SVE vs nSVE; intersection of pink and green sets). Points show each animal's gene expression count with bars denoting mean value ± SEM (q value <0.05 = *, <0.01 = **, <0.005 = ***, <0.001 = ****, with Benjamini-Hochberg correction, *Vipr2*$^{+/+}$ nSVE n=4, *Vipr2*$^{-/-}$ nSVE n=3, *Vipr2*$^{+/+}$ SVE n=4, *Vipr2*$^{-/-}$ SVE n=3).

exercise and the resultant altered profile in ingestive and locomotor activity does affect the SCN transcriptome of *Vipr2*$^{-/-}$ mice. For example, enrichment of the GO terms 'regulation of epithelial cell proliferation', 'insulin secretion', and 'peptide hormone secretion' were found in this comparison of SVE *Vipr2*$^{-/-}$ vs nSVE *Vipr2*$^{+/+}$ SCN gene expression. KEGG pathway analysis indicates that 'Prion disease', 'Huntington disease', and 'Parkinson disease' were among the terms downregulated in SVE *Vipr2*$^{-/-}$ mice, whereas 'Axon guidance', 'GABAergic synapse', and 'Retrograde endocannabinoid signaling' were among the terms upregulated in these animals. Therefore, some genotype differences in the SCN transcriptome are sustained under timed exercise conditions, whereas other genes and pathways such as those associated with neurodegenerative diseases are altered.

Timed-exercise does not alter widespread down-regulation of circadian-regulating factors and neuropeptides in the *Vipr2*$^{-/-}$ SCN

We next sought to identify subsets of genes that showed consistent differences in expression over different combinations of genotype and exercise comparisons. We focused on two groupings, one in which genotype differences in gene expression were consistent between SVE and nSVE conditions and the second where SVE upregulated genes in *Vipr2*$^{-/-}$ but not *Vipr2*$^{+/+}$ animals. For the first group, we found 43 genes whose expression was consistently different between *Vipr2*$^{+/+}$ and *Vipr2*$^{-/-}$ mice at CT14 of the nSVE condition and ZT14 of the SVE condition (Figure 4A). This includes genes considered above as well as others not previously discussed. For example, neuronatin (*Nnat*) is important for ion channel expression in the developing nervous system,[55] whereas *Sox3* is a transcription factor involved in embryonic brain development.[56] In tissues sampled at CT14 of the nSVE condition and ZT14 of the SVE condition, both *Nnat* and *Sox-3* were downregulated in *Vipr2*$^{-/-}$ compared to the *Vipr2*$^{+/+}$ mice. Similarly, VGF nerve growth factor inducible (*Vgf*) is downregulated in the *Vipr2*$^{-/-}$ SCN. This same pattern of higher levels in *Vipr2*$^{+/+}$ than *Vipr2*$^{-/-}$ tissue at both CT14 of the nSVE condition and ZT14 of the SVE condition was also observed for *Avp*, *Sst*, *Gpr176*, *Creb3l1*, and *C1ql3*. The opposite genotype difference was seen for *Penk* and *Ddc* (an enzyme involved in dopamine, serotonin and histamine processing). Compared to

Vipr2$^{+/+}$ tissue samples, both *Penk* and *Ddc* were upregulated in the *Vipr2*$^{-/-}$ SCN at CT14 of the nSVE and ZT14 of the SVE condition. The up-regulation of these transcripts in the *Vipr2*$^{-/-}$ SCN is consistent with the up-regulation in the addiction/reward processes identified by KEGG (Figure 3B). Therefore, many genotype differences in gene expression are sustained across circadian time points and exercise conditions and this includes neuropeptides and transcription factors.

For the second group, 38 genes were found to be dysregulated in the *Vipr2*$^{-/-}$ compared to *Vipr2*$^{+/+}$ SCN at CT14 of the nSVE condition, with SVE altering their expression in the *Vipr2*$^{-/-}$ but not *Vipr2*$^{+/+}$ animals (Figure 4B). This includes factors implicated in regulation of SCN circadian timekeeping (*Ncor1*)[35] chromatin remodeling (*Banp*)[48] and carcinoma (nuclear apoptosis-inducing factor 1; *Naif1* and *Kdr*).[57,58] Notably, core clock genes were not in this grouping. Thus, timed exercise can restore the expression of some genes in the *Vipr2*$^{-/-}$ SCN to near *Vipr2*$^{+/+}$ like levels, but this does not extend to core circadian clock genes. Other groupings of genes showing similar patterns of genotype and/or exercise-related changes in expression were found, but are not discussed further (see Figure S5).

Scheduled exercise restores behavioral rhythms without rescuing the *Vipr2*$^{-/-}$ SCN molecular Clock—qRT-PCR analysis

Three consecutive weeks of the SVE protocol alters the temporal profile of wheel-running and ingestive behavior of *Vipr2*$^{-/-}$ mice. Previously, we showed that this is accompanied by increases in *Vipr2*$^{-/-}$ SCN clock cell synchrony and restoration ~24h behavioral rhythmicity when the animals can free-run in constant dark at the termination of the exercise regimen[21,22] (also see Figure 6A). Here, using RNA-seq, we did not find any exercise-related alteration in the level of expression of components of the molecular clock in the *Vipr2*$^{-/-}$ SCN. To confirm and extend the limited temporal sampling of our RNA-seq approach, we used qRT-PCR to measure gene expression in a different cohort of *Vipr2*$^{+/+}$ and *Vipr2*$^{-/-}$ mice. We took SCN tissue (as well as liver and lung samples—see below) from *Vipr2*$^{-/-}$ mice at CT0 and CT14 of the nSVE condition and ZT14 of the SVE condition (see Figure 1). Furthermore, we took SCN tissue from *Vipr2*$^{+/+}$ animals at CT0 and CT14 of the nSVE condition and in *Vipr2*$^{+/+}$ mice showing entrainment to SVE, we assessed SCN tissue taken at CT14 as well as ZT14/CT22. We quantified the transcription levels of three core circadian clock components (*Arntl, Per2, and Nr1d1*), an SCN output factor (*Avp*), and one SCN gene known to be responsive to non-photic stimuli, the melanocortin receptor 3 (*Mc3r*).[59] We also quantified the neuropeptide prokineticin 2 (*Prok2*) as this is implicated as a key SCN output factor,[60] its expression in RNA-seq was found to be highly variable between replicates, especially in *Vipr2*$^{-/-}$ SCN samples, causing its p value to be below 0.05.

In the nSVE condition, none of the transcripts measured in the SCN of behaviorally rhythmic *Vipr2*$^{-/-}$ mice differed in expression between CT0 and CT14 (Figures 5A and 5B), whereas in *Vipr2*$^{+/+}$ mice, two core molecular clock components (*Per2* and *Nr1d1*), a non-photically responsive G-neuropeptide receptor (*Mc3r*), and the SCN output genes (*Avp* and *Prok2*), showed large changes consistent with the known temporal profiles of these transcripts in the neurochemically intact SCN.[60,61] *Arntl* did not change in expression in the *Vipr2*$^{+/+}$ nSVE SCN, presumably reflecting its intermediate levels of expression at these timepoints. The temporal expression of *Mc3r* in the SCN has not previously been reported and these novel findings suggest that *Mc3r* expression is regulated by the SCN molecular clockworks.

Consistent with and extending on the RNA-seq data, at CT14 of the nSVE condition, expression of two molecular clock components (*Arntl* and *Per2*), and SCN output genes (*Avp* and *Prok2*) was significantly lower in the *Vipr2*$^{-/-}$ compared with the *Vipr2*$^{+/+}$ SCN, whereas *Nr1d1* was significantly higher (Figures 5A and 5B). This builds on a previous report of damped molecular clock gene and *Avp* expression in the *Vipr2*$^{-/-}$ SCN[12] and further indicates that a key SCN output factor, *Prok2*, is also profoundly blunted in expression in these animals. Expression of *Mc3r* did not differ between the genotypes at CT14 of the nSVE condition and its expression in the *Vipr2*$^{-/-}$ SCN did not vary across nSVE timepoints, though this may reflect greater inter-individual variability between *Vipr2*$^{-/-}$ samples than for *Vipr2*$^{+/+}$. In the *Vipr2*$^{-/-}$ SCN, none of these transcripts (*Arntl*, *Per2*, *Nr1d1*, *Avp*, *Prok2*, and *Mc3r*) differed in expression at the SVE sample point compared with the nSVE timepoints. These measurements using qRT-PCR are broadly consistent with those of our RNA-seq investigation and, highlight that in behaviorally rhythmic *Vipr2*$^{-/-}$ animals (albeit with weaker rhythms more variable in circadian period than those of *Vipr2*$^{+/+}$ mice), genes for the molecular clock, clock output, and an arousal responsive G-protein coupled receptor are dysregulated. As timed-exercise evokes substantive changes in the temporal profile of wheel-running and ingestive behavior in

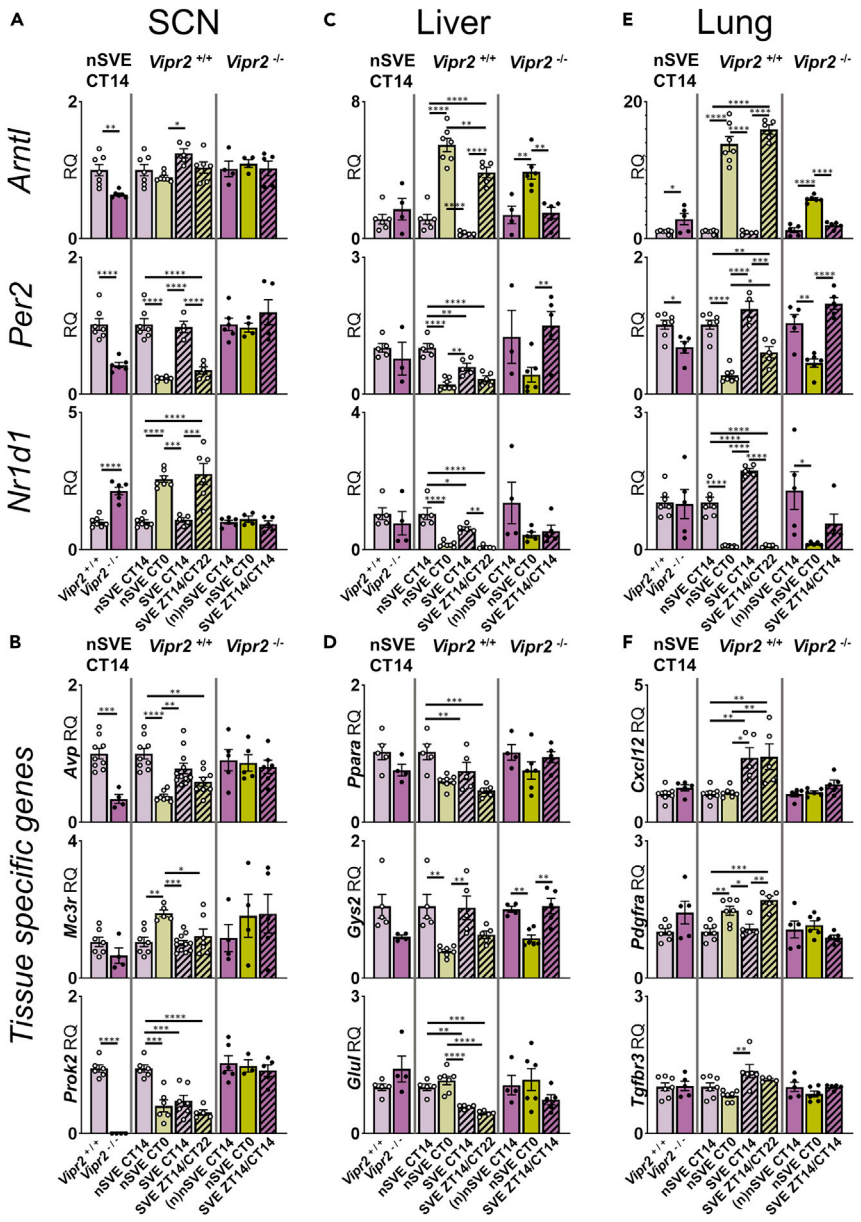

Figure 5. qRT-PCR quantification in the Suprachiasmatic nuclei, liver and lung

(A) Suprachiasmatic nuclei (SCN), (B) liver, and (C) lung qRT-PCR gene expression of clock genes (*Bmal1, Per2, Rev-ErbA)* and tissue specific genes *(Avp, Mc3r* and *Prok2* for (B) SCN; *Ppara, Gys2,* and *Glul* for (D) liver; *Cxcl12, Pdgfra* and *Tgfbr3* for (F) lung) in *Vipr2*$^{+/+}$ and *Vipr2*$^{-/-}$ mice, in nSVE and SVE conditions. Gene expression counts are normalized to the average of the data points in the first bar (*Vipr2*$^{+/+}$ nSVE CT14 for groups one and two, *Vipr2*$^{-/-}$ nSVE CT14 for the third column), the normalized values of nSVE CT14 are indicated with the prefix (n). Points show each animal's gene expression count with bars denoting mean value ± SEM (ANOVA and Tukey's *a priori* post-hoc test, p value <0.05 = *, <0.01 = **, <0.005 = ***, <0.001 = ****, sample sizes ranged from n=3 to n=11; individual data points are plotted in the figure).

Vipr2$^{-/-}$ mice (Figure 2B), it is surprising that this is not accompanied by overt changes in these dysregulated molecular programs of the *Vipr2*$^{-/-}$ SCN.

In *Vipr2*$^{+/+}$ mice, SVE causes small changes in circadian period and a moderate reduction in rhythm strength,[21,22] but unsurprisingly, the molecular clock activity was sustained in these animals: *Per2* and *Nr1d1* varying in expression between SVE timepoints and unaltered in comparison to CT0 and CT14 of the nSVE condition (Figure 5A). Furthermore, *Arntl* expression was elevated at SVE ZT14 compared with

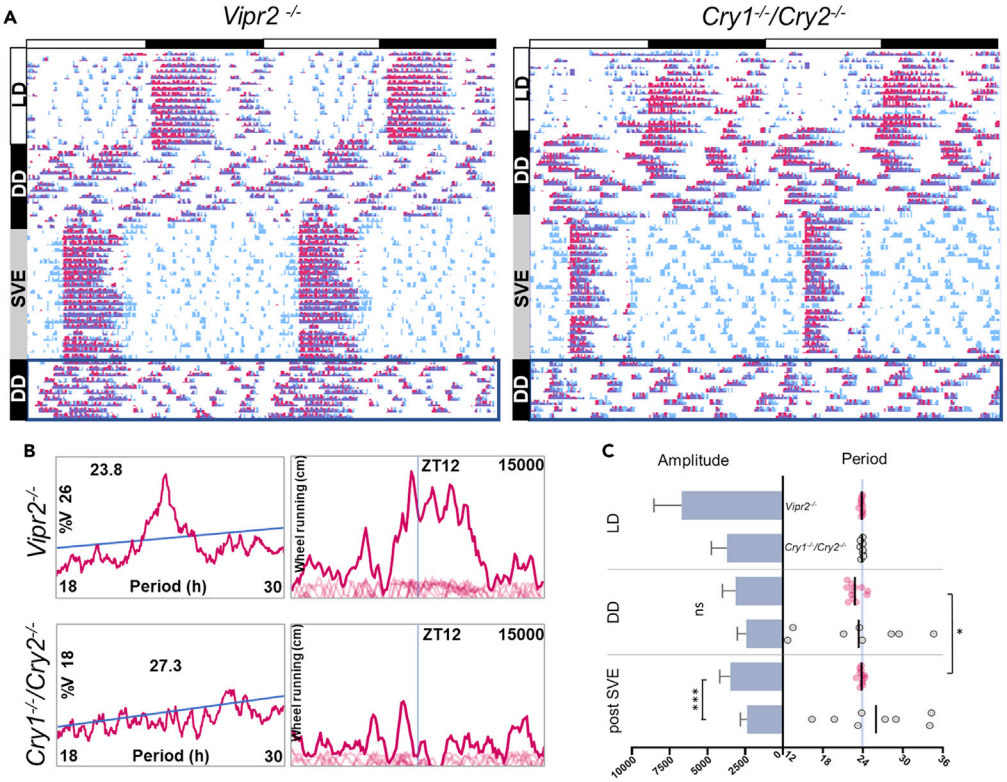

Figure 6. Mice lacking a functional molecular clock do not sustain 24h behavioral rhythms following scheduled voluntary exercise

(A) Double plotted actograms showing wheel running (pink) and drinking (blue) in exemplar *Vipr2*$^{-/-}$ and *Cry1*$^{-/-}$/*Cry2*$^{-/-}$mice. After two weeks in light-dark condition (LD), the lights were left off and the mice kept in constant dark (DD) for the remainder of the experiment. Following 2 weeks in DD, animals were placed on a scheduled voluntary exercise regimen (6h/24h; SVE) for three weeks and then put back in *ad libitum* running regime for the remainder of the experiment. Horizontal black/white bar = LD cycle in the first two weeks.

(B) Periodograms show the main frequency of wheel-running immediately after SVE (average value of the last 10 days of recording (blue box, % V = percentage of variance, blue line = significance threshold; $p<0.05$), of the actograms above. To the right of the periodograms, the profile plots depict the cumulative value (distance; in cm) of wheel running in each 10-min time bin in a 24-h period, for 10 consecutive days following SVE (single day values are in pale pink). ZT12 indicates the onset of wheel availability in the days before.

(C) Average amplitude (horizontal bars), and period (individual values: circles, vertical line: mean value in different experimental conditions in *Vipr2*$^{-/-}$(n = 8) and *Cry1*$^{-/-}$/*Cry2*$^{-/-}$(n = 13) mice. In contrast to *Cry1*$^{-/-}$/*Cry2*$^{-/-}$ animals, *Vipr2*$^{-/-}$ mice sustain near 24-h rhythms following SVE. For amplitude, unpaired t-test, *** = $p<0.001$; for period, paired t-test, * = $p<0.05$.

nSVE CT14, suggesting that this arm of the molecular clock was enhanced by timed exercise. However, unlike the nSVE condition, expression of *Avp* and *Prok2* in the *Vipr2*$^{+/+}$ SCN did not differ between SVE timepoints (Figure 5B), suggesting that suppressed *Vipr2*$^{+/+}$ clock output accompanies reduced behavioral rhythm strength previously observed following scheduled exercise.[21,22] Because in comparison to nSVE CT0, *Mc3r* expression is also reduced at SVE ZT14/CT22, then scheduled exercise may evoke more extensive alterations in *Vipr2*$^{+/+}$ SCN transcript profiles.

Circadian rhythms in peripheral oscillators of the *Vipr2*$^{-/-}$ mouse are intact

We next investigated how peripheral oscillators are affected by SVE and the loss of the $VPAC_2$ receptor. To do this, we used qRT-PCR and quantified transcript expression of *Arntl*, *Per2*, and *Nr1d1* and some physiologically relevant factors in the liver and lung. The liver is reported to have little/no $VPAC_2$ expression, whereas the lung has high expression.[62] This thus enables insight into potential contributions of VIP-$VPAC_2$ receptor signaling to peripheral molecular programs and their response to timed-exercise.

In the liver of *Vipr2*$^{+/+}$ mice, as expected, the expression of *Arntl*, *Per2*, and *Nr1d1* varied from nSVE CT0 to CT14. In response to SVE, expression of *Arntl*, *Per2*, and *Nr1d1* in the *Vipr2*$^{+/+}$ liver continued to vary over time but was blunted compared to the nSVE condition (Figure 5C). In the *Vipr2*$^{-/-}$ liver, the molecular clock was partially altered, with evidence of variation in expression of *Arntl* (but not *Per2*, and *Nr1d1*) between nSVE CT0 to CT14 and did not differ from that of the *Vipr2*$^{+/+}$ liver at CT14 of the nSVE condition. In response to SVE, *Per2* at ZT14 now differed from nSVE CT0, whereas *Nr1d1* did not. Thus, with loss of the $VPAC_2$ receptor, the molecular clock is partially intact and its response to timed exercise may be subtly altered.

We additionally profiled three physiologically relevant genes expressed in liver.[63,64] Glutamine synthetase (*Glul*) is important for removal of ammonia and peroxisome proliferator activated receptor alpha (*Pparα*) is a regulator of energy metabolism. Expression of neither *Glul* nor *Pparα* differed between nSVE timepoints in either *Vipr2*$^{+/+}$ or *Vipr2*$^{-/-}$ liver samples and neither differed between genotypes at CT14 (Figure 5D). When exposed to the SVE regimen, expression of both *Glul* and *Pparα* in *Vipr2*$^{+/+}$ liver was significantly lower at both timepoints than in nSVE samples, whereas expression in the *Vipr2*$^{-/-}$ liver did not change in response to timed exercise. This suggests that timed exercise suppresses *Glul* and *Pparα* in the *Vipr2*$^{+/+}$ but not the *Vipr2*$^{-/-}$ mouse liver. Expression of glycogen synthase 2 (*Gys2*) varied between CT14 and 0 in the nSVE condition in both genotypes and did not differ between liver samples from *Vipr2*$^{+/+}$ and *Vipr2*$^{-/-}$ liver at CT14. In response to SVE, the pattern of *Gys2* expression in *Vipr2*$^{+/+}$ mice remained similar to that observed under nSVE, in both genotypes. When considered together, these qRT-PCR assessments indicate differential effects of the loss of the $VPAC_2$ receptor on the expression of physiologically relevant genes in the liver, and no alteration of these by scheduled exercise. As $VPAC_2$ expression is minimal in the liver,[62] then these alterations in the molecular programs of the liver presumably arise indirectly from aberrant SCN output as well as changes in the temporal pattern of food intake.

$VPAC_2$ binding sites are present in the *Vipr2*$^{+/+}$ mouse lung and absent in lung of *Vipr2*$^{-/-}$ mice.[62] In the nSVE condition, molecular clock components (*Arntl*, *Per2*, and *Nr1d1*) altered in expression from CT14 to 0 in both genotypes, with *Arntl* being higher and *Per2* lower in the *Vipr2*$^{-/-}$ compared to the *Vipr2*$^{+/+}$ lung at CT14 (Figure 5E). This pattern of clock gene expression in the *Vipr2*$^{+/+}$ lung is consistent with previous findings[64] and further suggests that the lung molecular circadian clock is intact in *Vipr2*$^{-/-}$ animals. SVE did not alter expression of *Nr1d1* in the *Vipr2*$^{+/+}$ lung, but may suppress *Nr1d1* in the *Vipr2*$^{-/-}$ lung. Therefore, the lung circadian clock is sustained in the absence of local VIP-$VPAC_2$ signaling and is potentially altered by timed exercise.

C-X-C chemokine ligand 12 (*Cxcl12*) and transforming growth factor β receptor type III (*Tgfbr3*) are involved in fibrosis and carcinoma respectively and are expressed in the mouse lung.[31,64] Expression of neither *Cxcl12* nor *Tgfbr3* varied between *Vipr2*$^{+/+}$ and *Vipr2*$^{-/-}$ lungs sampled at nSVE CT14 and in neither genotype did expression of either of these vary between nSVE timepoints. Platelet growth factor receptor alpha (*Pdfgra*) is involved in myofibroblasts and here in *Vipr2*$^{+/+}$ lung its expression varied between CT14 and 0 in nSVE samples, but this time-of-day difference in expression was absent in the nSVE *Vipr2*$^{-/-}$ lung. Timed exercise upregulated *Cxcl12* expression in the *Vipr2*$^{+/+}$ lung at both timepoints, but did not change its expression in *Vipr2*$^{-/-}$ lung (Figure 5F), whereas neither *Tgfbr3* nor *Pdfgra* were altered by SVE in either the *Vipr2*$^{+/+}$ or *Vipr2*$^{-/-}$ lung. Collectively, from these findings we deduce that in *Vipr2*$^{+/+}$ lung, *Pdfgra* is potentially under circadian clock control. However, exercise-induced elevation in *Cxcl12* is not detected in the *Vipr2*$^{-/-}$ lung. Thus the absence of the $VPAC_2$ receptor potentially alters the response of the lung to exercise as well as fibrosis and other pathologies.

A molecular clock is necessary for scheduled exercise to promote 24h rhythms

Our observations that SVE does not noticeably alter the diminished circadian clock gene expression in the *Vipr2*$^{-/-}$ SCN raise the possibility that these period stabilizing and lengthening actions of SVE occur independently of the molecular circadian clock. To explore this possibility, we assessed how SVE influenced behavioral rhythms in *Cry1*$^{-/-}$*Cry2*$^{-/-}$ mice which lack a functional molecular clock in all tissues[65–67] and compared their behavioral parameters to those of a cohort of *Vipr2*$^{-/-}$ animals subject to the same protocols.[22] Under LD conditions, both *Vipr2*$^{-/-}$ and *Cry1*$^{-/-}$*Cry2*$^{-/-}$ mice synchronized to lights-off and exhibited 24h rhythms (Figure 6), but when transferred into DD, behaviorally rhythmic *Vipr2*$^{-/-}$ animals exhibit ~22.1h period in wheel-running activity (range: 21–24.5h), whereas *Cry1*$^{-/-}$*Cry2*$^{-/-}$ mice showed a broad range (~12.1–35.8h) in the period of very weak oscillations in wheel-running activity (Figure 6). With the

onset of timed-exercise, mice of both genotypes rapidly align the onset of drinking activity (~1–3 days) to the opportunity to exercise in the wheel, but on the termination of the SVE regimen, *Vipr2*$^{-/-}$ mice free-run with ~24h rhythms, whereas *Cry1*$^{-/-}$*Cry2*$^{-/-}$ animals exhibit a broad range of very weak rhythms (~17–34h) that cannot be distinguished from pre-SVE behavior. These observations indicate that although the absence of a molecular clock does not impede behavioral alignment to timed exercise, a functional molecular clock is necessary to sustain 24h rhythms after the scheduled exercise is ended. This is consistent with our previous data from longitudinal studies in which we found SVE to improve synchrony among *Vipr2*$^{-/-}$ SCN clock cells.[21] An intriguing but untested possibility is that a minimally functional SCN molecular clock can support behavioral rhythms in locomotor and ingestive behavior.

E-boxes and CREs are common in differentially expressed genes in the *Vipr2*$^{-/-}$ SCN

Because a functional molecular clock is necessary for the promotion of 24h behavioral rhythms and because the $VPAC_2$ receptor is positively coupled to adenylate cyclase[38,68] we hypothesized that genes with cyclicAMP response elements (CREs; to which cyclicAMP response element binding proteins or CREBs bind) and/or E-boxes (to which the ARNTL binds) in their promoter regions are predisposed to being affected by the loss of the $VPAC_2$ receptor. To explore this, we interrogated the JASPAR database[69] to examine a subset of differentially expressed genes for predicted CRE- and/or E-boxes in their promoter regions. We found that in the mouse database, the genes *Avp*, *Banp*, *C1ql3*, *Cck*, *Creb3l1*, *Gpr176*, *Kctd18*, *Mobp*, and *Ncor1* were predicted to have E-boxes (Figure 7), whereas *Gpr176*, *Kctd18*, *Mobp*, *Banp*, *Comt*, *Creb3l1*, *Kdr*, *Mobp*, *Naif1*, *Ncor1*, *Pdyn*, *Penk*, *Snca*, *Sst*, *Vgf*, and *Vip* were predicted to have CREs (Figure 7). Many, but not all of these genes vary in expression over 24 h in the mouse SCN.[70] Interrogation of the JASPAR human database also identified many of the same genes (and more). Because we observed down-regulation of *Avp*, *Vip*, *Sst*, *Gpr176*, *C1ql3*, *Banp*, *Creb3l1*, *Mobp*, *Naif1*, *Ncor1*, *Kdr*, and *Kctd18*, as well as up-regulation of *Gpc3*, *Scna*, *Pdyn*, and *Penk* in the *Vipr2*$^{-/-}$ SCN, this indicates differential consequences for gene expression arising from loss in VIP-$VPAC_2$ receptor signaling and suggests potential candidates that timed exercise engages within the *Vipr2*$^{-/-}$ SCN to promote 24 h rhythms.

DISCUSSION

By convention, circadian rhythms in behavior including wheel-running and ingestive activity are attributed to the SCN molecular circadian clock driving ~24h rhythms in SCN cellular activity and chemical communication. Here, in the SCN of *Vipr2*$^{-/-}$ mice behaviorally rhythmic in the nSVE condition, we do not observe the early day-early night changes in the molecular clock seen in the SCN of behaviorally rhythmic *Vipr2*$^{+/+}$ mice. Clock gene expression was altered in these *Vipr2*$^{-/-}$ mouse, with *Per2* and *Arntl* downregulated and *Nr1d1* upregulated. Surprisingly, expression of a broad range of SCN neuropeptides (*Sst*, *Pdyn*, *Penk*, and *Vip*) including those involved in communication of circadian information to the rest of the brain and body (*Avp* and *Prok2*) was dysregulated in the SCN of these behaviorally rhythmic *Vipr2*$^{-/-}$ animals. Further, although three weeks of SVE alters the 24h profile of food and water intake and improves *Vipr2*$^{-/-}$ SCN clock cell synchrony to promote ~24h behavioral rhythms in these mice,[21] we did not detect changes (increase or decrease) in the expression of any component of the *Vipr2*$^{-/-}$ SCN molecular clock nor did we observe correction in SCN neuropeptide expression. The behavioral rhythms of *Vipr2*$^{+/+}$ mice are slightly weakened by SVE and although their SCN molecular clock does not appear to be altered by SVE, the expression of SCN output factors, *Avp* and *Prok2*, is reduced. Therefore, the SCN molecular clock of *Vipr2*$^{+/+}$ mice and its response to the non-photic zeitgeber of scheduled exercise functions in accordance with current understanding,[71] whereas that of *Vipr2*$^{-/-}$ animals does not. Consistent with this, KEGG pathway analysis indicated a broad range of SCN transcriptomic changes between genotypes and exercise conditions. In contrast, the liver and lung peripheral oscillators and their molecular response to timed exercise appear much less affected by the loss of the $VPAC_2$ receptor.

The transcriptome of single cells in the mouse SCN has been recently profiled[72–74] and based in part on the differential expression of neuropeptides, 5 neuronal clusters have been deduced[73]: 1) *Avp*$^{+}$/*Nms*$^{+}$, 2) *Vip*$^{+}$/*Nms*$^{+}$, 3) *Vip*$^{+}$/*Grp*$^{+}$, 4) *Cck*$^{+}$/*C1ql3*$^{+}$, and 5) *Cck*$^{+}$/*Bdnf*$^{+}$. Mapping of the neuroanatomical distribution of these clusters reveals that although there is some overlap, they delineate different anatomical regions of the SCN.[73,75,76] Our observation of dysregulation of *Avp*, *Vip*, and *C1ql3* as well as *Sst* and *Vgf* in the *Vipr2*$^{-/-}$ SCN suggests that the loss of the $VPAC_2$ receptor alters transcriptional programs throughout the SCN. This is consistent with the widespread expression of the $VPAC_2$ receptor in the rodent SCN.[77–79]

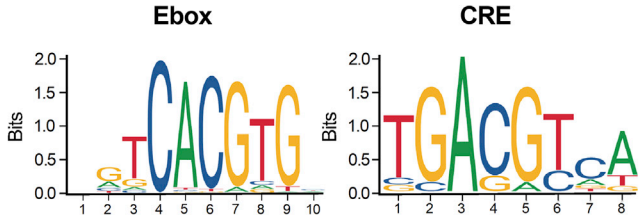

JASPAR Species Database	Binding Site				*Vipr2*$^{-/-}$ nSVE vs. *Vipr2*$^{+/+}$nSVE Log2FC	*Varies over 24h*
	ARNTL		CREB1			
	Mouse	Human	Mouse	Human		
Gene						
Avp	√	√		√	↓	√
Banp	√		√	√	↓	√
C1ql3	√			√	↓↓	√
Cck	√	√		√	ns	–
Comt		√	√		ns	–
Creb3l1	√		√		↓↓	√
Ddc		√		√	↑	√
Gpc3		√		√	↑↑	–
Gpr176	√	√	√		↓	–
Kctd18	√	√			↓↓	–
Kdr			√		↓↓	–
Miat					ns	n/a
Mobp	√		√		↓↓	–
Naif1		√	√	√	↓	–
Ncor1	√		√	√	↓	–
Ndufa4		√		√	ns	√
Nnat				√	↓↓	√
Pdyn		√	√		↑↑	–
Penk			√	√	↑	√
Rgs16		√			ns	√
Snca			√		↑	√
Sox3			√		↓	√
Sst			√	√	↓	–
Vgf		√	√	√	↓	√
Vip			√	√	↓	√

Figure 7. E-boxes and CREs are present in many dysregulated genes in the *Vipr2*$^{-/-}$ SCN

Many genes that are dysregulated in the *Vipr2*$^{-/-}$ SCN are predicted to contain cyclicAMP response elements (CREs; to which cyclicAMP response element binding proteins or CREBs bind) and/or E-boxes (to which the ARNTL binds) in their promoter regions. Log2FC ↑= 0 to 1, ↑↑= 1 to 2, ↓ = 0 to −1, ↓↓ = −1 to −2, ns= non-significant. √ predicted in the JASPAR database. To identify which genes vary in expression over 24h (√), we consulted a mouse SCN RNA-seq database (http://www.wgpembroke.com ⟩ shiny ⟩ SCNseq) that was established by Pembroke et al.[70.]

Concordant with this, GABA is synthesized by most if not all SCN neurons.[80] This neurotransmitter plays important roles in circadian timing[81] including influencing intercellular synchrony in the SCN[82,83] the amplitude of SCN circadian rhythms,[84] and the phasing of neuronal and molecular activity in the SCN.[85] Here, in comparison to *Vipr2*$^{+/+}$ mice, the KEGG term 'GABAergic synapse' was upregulated in the *Vipr2*$^{-/-}$ SCN in both nSVE and SVE conditions (Figures 3B and 3H). Previously under nSVE conditions we found that the response of SCN neurons to a $GABA_A$ receptor antagonist was reduced in the *Vipr2*$^{-/-}$ compared *Vipr2*$^{+/+}$ SCN and that SVE further attenuated this response in the *Vipr2*$^{-/-}$ SCN.[21] This suggests that GABAergic neurotransmission is altered both by the loss of the $VPAC_2$ receptor as well as timed daily exercise. Determining precisely how these alterations in GABA signaling arise will require further research.

The unexpectedly wide range of neuropeptide genes downregulated in the *Vipr2*$^{-/-}$ SCN could arise from dysregulation of transcription factors (Figures 3A and 4A). For example, CREB3l1 is implicated in AVP synthesis[39] and *Creb3l1* is also downregulated in the *Vipr2*$^{-/-}$ SCN. As CREB3l1 may also factor in the transport of neuropeptides to synaptic terminals,[86] then diminution in its expression could both reduce neuropeptide gene activation as well as neuropeptide release. It is not known if CREB3l1 influences the expression of other SCN neuropeptides, but the 'regulon' for *Creb3l1* is particularly enriched in *Avp*$^{+}$/*Nms*$^{+}$, *Vip*$^{+}$/*Nms*$^{+}$, and *Cck*$^{+}$/*C1ql3*$^{+}$ neurons and as noted above, *Avp*, *Vip*, and *C1ql3* are downregulated in the *Vipr2*$^{-/-}$ SCN, whereas *Nms*, *Cck*, *Grp* and *Bdnf* are not.[73] This indicates that co-expressed genes can be differentially regulated within SCN neurons. Consistent with this, we also observe that the opioid-related neuropeptide genes, *Penk* and *Pdyn* are upregulated in the *Vipr2*$^{-/-}$ SCN (Figures 3A and S5H). Furthermore, fast neurochemical signals are also potentially changed by loss of the $VPAC_2$ receptor. For example, dopa decarboxylase (*Ddc*) which catalyzes DOPA to dopamine, 5-hydroxytryptophan to serotonin, and histidine to histamine was also upregulated in the *Vipr2*$^{-/-}$ SCN. In addition, other factors that influence circadian rhythms in behavior including *Gpr176* and *Ncor1* are dysregulated in the *Vipr2*$^{-/-}$ SCN (Figure 4). Thus, despite widespread alterations in the SCN transcriptome, including that of transcription factors, key neuropeptides and neurochemical signals, *Vipr2*$^{-/-}$ mice can exhibit circadian rhythms in behavior, both before and following timed-exercise.

Another influence on the SCN transcriptome is neuronal activity. Neurons of the SCN exhibit a pronounced circadian rhythm in activity, being more depolarized and firing more action potentials during the day than the night.[87,88] Targeted impairment of neuronal activity in the SCN desynchronizes SCN clock cell synchrony and blunts the rhythms in molecular clock gene expression.[12,89–91] Furthermore, neuropeptide transcription, for instance *Avp*, can be impaired by the loss of SCN intercellular communication.[92] In this regard, neurons of the *Vipr2*$^{-/-}$ SCN are more hyperpolarized[40] and spontaneously discharge action potentials at a lower frequency than SCN neurons of *Vipr2*$^{+/+}$ mice, particularly in the ventral subregion of the SCN.[21,41] This hypoactivity likely arises from changes in ion channel expression and notably *Kcnc2* which codes for *Kv3.2*, a potassium channel subunit important for SCN neuronal excitability,[42] is downregulated in the *Vipr2*$^{-/-}$ SCN. Therefore, diminished neuronal activity could also reinforce dysregulation of the molecular clock and neuropeptide gene expression in the *Vipr2*$^{-/-}$ mice.[87]

The period of circadian oscillators can be altered by DNA methylation and chromatin remodeling.[93] Environmental stimuli can alter the methylated state of SCN circadian clock genes and change the period of behavioral rhythms.[94] Here, we did not observe systematic changes in expression of DNA methyltransferase-related genes (*Kdm2a*, *Jmjd1c*, *Dnmt1*, *Dnmt3a*, *Dnmt3b*, and *Dnmt3l*) or demethylation tet-eleven translocation genes (*Tet1*, *Tet2*, and *Tet3*) that are known to be present in the mouse SCN.[94] However, *Banp* is upregulated by SVE in the *Vipr2*$^{-/-}$ SCN (Figures 3E and 4B) and BANP can open chromatin and activate CpG-island regulated genes.[48] Similarly, *Ncor1*, nuclear co-repressor receptor 1, can interact with *histone deacetylase 3 (Hdac3)*[95] and in genetically modified mice in which NCOR1 cannot interact with HDAC3, the circadian period of behavioral rhythms is shortened by ~0.4h.[96] Furthermore, NCOR1 can interact with methyl-CpG-binding protein 2 (MeCP2)[97] as well as NR1D1.[98,99] Here, in the nSVE condition, *Ncor1* is downregulated in the *Vipr2*$^{-/-}$ compared with *Vipr2*$^{+/+}$ SCN (Figure 4B), with SVE up-regulating its expression the *Vipr2*$^{-/-}$ SCN. Therefore, exercise-evoked chromatin remodeling and epigenetic regulation of specific genes are potential contributors to the period altering effects of loss of the $VPAC_2$ receptor as well as the period lengthening actions of timed exercise in the *Vipr2*$^{-/-}$ animals.

It is becoming increasingly apparent that there is functional redundancy in the molecular clock as well as for neurochemical signals of the SCN. For example, given the importance of VIP-$VPAC_2$ signaling to the SCN and the expression of behavioral rhythms, in our previous study we crossbred *Vip*$^{-/-}$ and *Vipr2*$^{-/-}$ mice to create *Vip*$^{-/-}$ *Vipr2*$^{-/-}$ animals. Surprisingly, some of these *Vip*$^{-/-}$ *Vipr2*$^{-/-}$ mice retain behavioral rhythmicity.[21] Similarly, Doi and colleagues created triple knockout mouse deficient in key neuropeptides (*Nmu* and *Nms*) and a G-protein coupled receptor (*Gpr176*) and the mice retained circadian rhythms in behavior.[100] Furthermore, it would be tempting to assume that simply knocking out *Bmal1* (*Arntl*) in $VPAC_2$ expressing cells of the SCN could abolish behavioral rhythms. However, such animals express a continuum of behavioral phenotypes, ranging from arrhythmic to near 24h rhythms.[101] Therefore, more studies are required to determine the necessity of the SCN for these actions of scheduled exercise on circadian rhythmicity in *Vipr2*$^{-/-}$ animals.

Indeed timed exercise could act on oscillators independent of the SCN. Rhythmic clock gene expression is observed in extra SCN sites across the rostrocaudal axis of the mammalian brain,[102–106] and for review see.[107,108] Furthermore, as noted in this and other investigations, some peripheral oscillators such as the lung, liver, and thyroid gland are functional in the *Vipr2*$^{-/-}$ animals.[90,109,110] It is possible that one or of more these or the coordinated activity among them is sufficient to organize and sustain 24h rhythms in behavior.[107]

In this regard, two circadian timekeepers that are well-characterized to promote SCN-independent behavioral rhythms are the food entrainable oscillator (FEO[111,112]) and methamphetamine sensitive circadian oscillator (MASCO[113]). The precise anatomical and/or neuroanatomical substrates of these are unclear but most likely involve a network of oscillators in the brain and the periphery. In rodents, the FEO is evoked when an animal is placed on restricted feeding schedule whereby most of its daily calories are presented early in the rest phase of successive circadian cycles.[114] Although the FEO can be activated this way in *Vipr2*$^{-/-}$ mice,[109] there is no food or calorie restriction in the nSVE and SVE conditions of this study. Similarly, the MASCO is activated through long-term administration of the additive psychostimulant metamphetamine, but no psychostimulant drugs are given to the animals in the nSVE or SVE components of this study. Because voluntary locomotory exercise in a running-wheel is ascribed as having rewarding properties[27,115] and because KEGG analysis indicates up-regulation of reward pathways in the *Vipr2*$^{-/-}$SCN (Figure 3B), then these mice may be more responsive to reward associated with timed exercise in a running-wheel. Further research is necessary to illuminate this possibility.

Limitations and conclusions of the study

The temporal resolution of the RNA-seq investigation is coarse and consequently, we cannot comment conclusively about circadian regulation of the SCN transcriptome. For economic reasons, we limited the sampling frequency, although we mitigate this to an extent with additional sampling times in the qRT-PCR component of the study. Nonetheless in our limited sampling, we found many transcriptomic differences in the SCN arising as a consequence of the loss of the $VPAC_2$ receptor and could confirm some changes using qRT-PCR. Furthermore, we also detected timed exercise alterations in the *Vipr2*$^{-/-}$ SCN transcriptome and observe that circadian oscillators in the liver and lung appear mostly intact in *Vipr2*$^{-/-}$ mice. A second limitation is that because we assess gene expression at the whole SCN level, we cannot comment authoritatively on the subregional variation in gene expression. However, our observation of down-regulation in *Avp*, *Vip*, and *Sst*, and corresponding up-regulation in *Penk* and *Pdyn* suggests differential subregional effects of the loss of $VPAC_2$ expression in the SCN (Figure 4A). In particular, *Penk* and *Pdyn* are mostly expressed in a different subpopulation of SCN neurons to those that synthesize *Avp* and *Vip*.[73] Therefore, our experimental design did not hinder us from making new observations on widespread genetic and exercise mediated changes in SCN transcriptome.

Collectively, our findings confirm that in animals lacking $VPAC_2$ receptor expression, scheduled voluntary exercise can readily entrain the onset of their intrinsic drinking rhythm to coincide with that of wheel availability. The transcriptomic profiling of these mice reveals that several key clock genes and neurochemical signaling pathways are dysregulated in their SCN, whereas molecular programs in their liver and lung are mostly intact. This indicates that other signals functioning independently of the $VPAC_2$ receptor enable cells of these tissues to synchronize. Intriguingly, although timed exercise lengthens the circadian period of behavior and alters the daily profile of ingestive and locomotor activity of *Vipr2*$^{-/-}$ mice to resemble that of neurochemically intact animals, this is not accompanied by corresponding changes in molecular clock genes or neurochemical signaling pathways in the SCN. It is not clear how this arousal-related cue accomplishes these pronounced behavioral corrections. Because we found that *Cry1*$^{-/-}$*Cry2*$^{-/-}$ mice cannot sustain the ~24h rhythms following timed-exercise, then this suggests a that a functional molecular is necessary for these actions SVE. It remains possible that a minimally functional SCN is able to orchestrate daily rhythms and to sustain long-term changes in circadian period in response to recurrent feedback from timed physical exercise. It is also possible that one or more extra-SCN brain structures and/or peripheral oscillators responds to regular physical exercise to shape and drive brain circuits that underpin ingestive and locomotor behaviors. Our findings confirm that scheduled physical exercise is an effective tool to improve 24h behavioral rhythms in a model of circadian timekeeping disruption, and further highlight the need to explore the brain sites and mechanisms of its action. Because circadian dysfunction and diminished neuropeptide expression in the human SCN is observed in aging[116] as well as in some neurodegenerative conditions,[117] then our study argues for continued research to determining the sites and molecular mechanisms underpinning the beneficial effects of physical exercise on the neural circadian system.

STAR★METHODS

Detailed methods are provided in the online version of this paper and include the following:

- KEY RESOURCES TABLE
- RESOURCE AVAILABILITY
  - Lead contact
  - Materials availability
  - Data and code availability
- EXPERIMENTAL MODEL AND SUBJECT DETAILS
- METHOD DETAILS
  - Quantitative RT-PCR
  - RNA-seq
- QUANTIFICATION AND STATISTICAL ANALYSIS

SUPPLEMENTAL INFORMATION

Supplemental information can be found online at https://doi.org/10.1016/j.isci.2023.106002.

ACKNOWLEDGEMENTS

TH, CP, NT, and ATLH were supported by project grantsupport to HDP from the Biotechnology and Biological Sciences Research Council (BBSRC; BB/M02239X/1 and BB/R019223/1 at the Universities of Manchester and Bristol). ATLH was supported by a Research Grant from The Physiological Society. J-MF is supported by an MRC Future Leaders Fellowship (MR/S031812/1). CM is supported by a BBSRC SWBio Doctoral Training Program studentship (BB/T008741/1). Some analysis originates from a thesis submitted by EC for an MSc in Bioinformatics. We thank Leo van Zeef and Andrew Hayes at the Core Genomics Facility at the University of Manchester for advice and technical assistance. We also thank Dr. Lukasz Chrobok for feedback on earlier drafts of the manuscript and Dr. Michael Greenwood for discussions on CREB3L1 function.

AUTHOR CONTRIBUTIONS

H.D.P., A.T.L.H., and C.P. designed the study. A.T.L.H., C.P., and N.T. collected tissue samples and performed the molecular assays. E.C. and J-M.F. performed bioinformatic analysis on the RNA-seq data. H.D.P., T.H., and C.M. analyzed behavioral and qRT PCR data. T.H. prepared the figures. T.H. and H.D.P. wrote the initial draft of the manuscript. A.T.L.H. and J-M.F. assisted in editing the manuscript.

DECLARATION OF INTERESTS

The authors declare no competing interests.

INCLUSION AND DIVERSITY

One or more of the authors of this manuscript self-identifies as a gender minority in their field of research. One or more of the authors of this manuscript self-identifies as a member of the LGBTQ+ community.

Received: September 6, 2022
Revised: November 25, 2022
Accepted: January 13, 2023
Published: February 17, 2023

REFERENCES

1. Hastings, M.H., Maywood, E.S., and Brancaccio, M. (2018). Generation of circadian rhythms in the suprachiasmatic nucleus. Nat. Rev. Neurosci. *19*, 453–469. https://doi.org/10.1038/S41583-018-0026-Z.

2. Brown, T.M. (2016). Using light to tell the time of day: sensory coding in the mammalian circadian visual network. J. Exp. Biol. *219*, 1779–1792. https://doi.org/10.1242/JEB.132167.

3. Mrosovsky, N. (1996). Locomotor activity and non-photic influences on circadian clocks. Biol. Rev. Camb. Philos. Soc. *71*, 343–372. https://doi.org/10.1111/J.1469-185X.1996.TB01278.X.

4. Mistlberger, R.E., and Antle, M.C. (2011). Entrainment of circadian clocks in mammals by arousal and food. Essays Biochem. *49*, 119–136. https://doi.org/10.1042/BSE0490119.

5. Hughes, A.T.L., and Piggins, H.D. (2012). Feedback actions of locomotor activity to the circadian clock. Prog. Brain Res. *199*, 305–336. https://doi.org/10.1016/B978-0-444-59427-3.00018-6.

6. Morin, L.P. (2013). Neuroanatomy of the extended circadian rhythm system. Exp. Neurol. *243*, 4–20. https://doi.org/10.1016/J.EXPNEUROL.2012.06.026.

7. Takahashi, J.S. (2017). Transcriptional architecture of the mammalian circadian clock. Nat. Rev. Genet. *18*, 164–179. https://doi.org/10.1038/NRG.2016.150.

8. Nosal, C., Ehlers, A., and Haspel, J.A. (2020). Why lungs keep time: circadian rhythms and lung immunity. Annu. Rev. Physiol. *82*, 391–412. https://doi.org/10.1146/ANNUREV-PHYSIOL-021119-034602.

9. Tahara, Y., and Shibata, S. (2016). Circadian rhythms of liver physiology and disease: experimental and clinical evidence. Nat. Rev. Gastroenterol. Hepatol. *13*, 217–226. https://doi.org/10.1038/NRGASTRO.2016.8.

10. Piggins, H.D., and Cutler, D.J. (2003). The roles of vasoactive intestinal polypeptide in the mammalian circadian clock. J. Endocrinol. *177*, 7–15. https://doi.org/10.1677/JOE.0.1770007.

11. Ono, D., Honma, K.I., and Honma, S. (2021). Roles of neuropeptides, VIP and AVP, in the mammalian central circadian clock. Front. Neurosci. *15*, 650154. https://doi.org/10.3389/FNINS.2021.650154.

12. Harmar, A.J., Marston, H.M., Shen, S., Spratt, C., West, K.M., Sheward, W.J., Morrison, C.F., Dorin, J.R., Piggins, H.D., Reubi, J.C., et al. (2002). The VPAC(2) receptor is essential for circadian function in the mouse suprachiasmatic nuclei. Cell *109*, 497–508. https://doi.org/10.1016/S0092-8674(02)00736-5.

13. Hughes, A.T., Fahey, B., Cutler, D.J., Coogan, A.N., and Piggins, H.D. (2004). Aberrant gating of photic input to the suprachiasmatic circadian pacemaker of mice lacking the VPAC2 receptor. J. Neurosci. *24*, 3522–3526. https://doi.org/10.1523/JNEUROSCI.5345-03.2004.

14. Pedersen, B.K. (2019). Physical activity and muscle-brain crosstalk. Nat. Rev. Endocrinol. *15*, 383–392. https://doi.org/10.1038/S41574-019-0174-X.

15. Deslandes, A., Moraes, H., Ferreira, C., Veiga, H., Silveira, H., Mouta, R., Pompeu, F.A.M.S., Coutinho, E.S.F., and Laks, J. (2009). Exercise and mental health: many reasons to move. Neuropsychobiology *59*, 191–198. https://doi.org/10.1159/000223730.

16. Meijer, J.H., and Robbers, Y. (2014). Wheel running in the wild. Proc. Biol. Sci. *281*, 20140210. https://doi.org/10.1098/RSPB.2014.0210.

17. Goh, J., and Ladiges, W. (2015). Voluntary wheel running in mice. Curr. Protoc. Mouse Biol. *5*, 283–290. https://doi.org/10.1002/9780470942390.MO140295.

18. Kumar, D., Soni, S.K., Kronfeld-Schor, N., and Singaravel, M. (2020). Wheel-running activity rhythms and masking responses in the diurnal palm squirrel, Funambulus pennantii. Chronobiol. Int. *37*, 1693–1708. https://doi.org/10.1080/07420528.2020.1826959.

19. Edgar, D.M., and Dement, W.C. (1991). Regularly scheduled voluntary exercise synchronizes the mouse circadian clock. Am. J. Physiol. *261*, R928–R933. https://doi.org/10.1152/AJPREGU.1991.261.4.R928.

20. Marchant, E.G., and Mistlberger, R.E. (1996). Entrainment and phase shifting of circadian rhythms in mice by forced treadmill running. Physiol. Behav. *60*, 657–663. https://doi.org/10.1016/S0031-9384(96)80045-X.

21. Hughes, A.T.L., Samuels, R.E., Baño-Otálora, B., Belle, M.D.C., Wegner, S., Guilding, C., Northeast, R.C., Loudon, A.S.I., Gigg, J., and Piggins, H.D. (2021). Timed daily exercise remodels circadian rhythms in mice. Commun. Biol. *4*, 761. https://doi.org/10.1038/s42003-021-02239-2.

22. Power, A., Hughes, A.T.L., Samuels, R.E., and Piggins, H.D. (2010). Rhythm-promoting actions of exercise in mice with deficient neuropeptide signaling. J. Biol. Rhythms *25*, 235–246. https://doi.org/10.1177/0748730410374446.

23. Hughes, A.T.L., and Piggins, H.D. (2008). Behavioral responses of Vipr2-/- mice to light. J. Biol. Rhythms *23*, 211–219. https://doi.org/10.1177/0748730408316290.

24. Porterfield, V.M., Piontkivska, H., and Mintz, E.M. (2007). Identification of novel light-induced genes in the suprachiasmatic nucleus. BMC Neurosci. *8*, 98. https://doi.org/10.1186/1471-2202-8-98.

25. Xu, P., Berto, S., Kulkarni, A., Jeong, B., Joseph, C., Cox, K.H., Greenberg, M.E., Kim, T.K., Konopka, G., and Takahashi, J.S. (2021). NPAS4 regulates the transcriptional response of the suprachiasmatic nucleus to light and circadian behavior. Neuron *109*, 3268–3282.e6. https://doi.org/10.1016/J.NEURON.2021.07.026.

26. Jagannath, A., Butler, R., Godinho, S.I.H., Couch, Y., Brown, L.A., Vasudevan, S.R., Flanagan, K.C., Anthony, D., Churchill, G.C., Wood, M.J.A., et al. (2013). The CRTC1-SIK1 pathway regulates entrainment of the circadian clock. Cell *154*, 1100–1111. https://doi.org/10.1016/J.CELL.2013.08.004.

27. Sherwin, C.M. (1998). Voluntary wheel running: a review and novel interpretation. Anim. Behav. *56*, 11–27. https://doi.org/10.1006/ANBE.1998.0836.

28. Davidson, A.J., Stokkan, K.A., Yamazaki, S., and Menaker, M. (2002). Food-anticipatory activity and liver per1-luc activity in diabetic transgenic rats. Physiol. Behav. *76*, 21–26. https://doi.org/10.1016/S0031-9384(02)00680-7.

29. Namvar, S., Gyte, A., Denn, M., Leighton, B., and Piggins, H.D. (2016). Dietary fat and corticosterone levels are contributing factors to meal anticipation. Am. J. Physiol. Regul. Integr. Comp. Physiol. *310*, R711–R723. https://doi.org/10.1152/AJPREGU.00308.2015.

30. Yasuda, S., Iwami, S., Tamura, K., Ikeda, Y., Kamagata, M., Sasaki, H., Haraguchi, A., Miyamatsu, M., Hanashi, S., Takato, Y., et al. (2019). Phase resetting of circadian peripheral clocks using human and rodent diets in mouse models of type 2 diabetes and chronic kidney disease. Chronobiol. Int. *36*, 851–869. https://doi.org/10.1080/07420528.2019.1594245.

31. Zhang, R., Lahens, N.F., Ballance, H.I., Hughes, M.E., and Hogenesch, J.B. (2014). A circadian gene expression atlas in mammals: implications for biology and medicine. Proc. Natl. Acad. Sci. USA *111*, 16219–16224. https://doi.org/10.1073/PNAS.1408886111.

32. Guo, M., Zhang, H., Zheng, J., and Liu, Y. (2020). Glypican-3: a new target for diagnosis and treatment of hepatocellular carcinoma. J. Cancer *11*, 2008–2021. https://doi.org/10.7150/JCA.39972.

33. Giatromanolaki, A., Koukourakis, M.I., Sivridis, E., Chlouverakis, G., Vourvouhaki, E., Turley, H., Harris, A.L., and Gatter, K.C. (2007). Activated vegfr2/kdr pathway in tumour cells and tumour associated vessels of colorectal cancer. Eur. J. Clin. Invest. *37*, 878–886. https://doi.org/10.1111/J.1365-2362.2007.01866.X.

34. Frederick, A., Goldsmith, J., de Zavalia, N., and Amir, S. (2017). Mapping the co-localization of the circadian proteins PER2 and BMAL1 with enkephalin and substance P throughout the rodent forebrain. PLoS One *12*, e0176279. https://doi.org/10.1371/JOURNAL.PONE.0176279.

35. Yin, L., and Lazar, M.A. (2005). The orphan nuclear receptor Rev-erbalpha recruits the N-CoR/histone deacetylase 3 corepressor to regulate the circadian Bmal1 gene. Mol. Endocrinol. *19*, 1452–1459. https://doi.org/10.1210/ME.2005-0057.

36. Chew, K.S., Fernandez, D.C., Hattar, S., Südhof, T.C., and Martinelli, D.C. (2017). Anatomical and behavioral investigation of C1ql3 in the mouse suprachiasmatic nucleus. J. Biol. Rhythms *32*, 222–236. https://doi.org/10.1177/0748730417704766.

37. Yoshikawa, T., Nakajima, Y., Yamada, Y., Enoki, R., Watanabe, K., Yamazaki, M., Sakimura, K., Honma, S., and Honma, K.i. (2015). Spatiotemporal profiles of arginine vasopressin transcription in cultured suprachiasmatic nucleus. Eur. J. Neurosci. *42*, 2678–2689. https://doi.org/10.1111/EJN.13061.

38. Langer, I., Jeandriens, J., Couvineau, A., Sanmukh, S., and Latek, D. (2022). Signal transduction by VIP and PACAP receptors. Biomedicines *10*, 406. https://doi.org/10.3390/BIOMEDICINES10020406.

39. Greenwood, M., Bordieri, L., Greenwood, M.P., Rosso Melo, M., Colombari, D.S.A., Colombari, E., Paton, J.F.R., and Murphy, D. (2014). Transcription factor CREB3L1 regulates vasopressin gene expression in the rat hypothalamus. J. Neurosci. *34*, 3810–3820. https://doi.org/10.1523/JNEUROSCI.4343-13.2014.

40. Pakhotin, P., Harmar, A.J., Verkhratsky, A., and Piggins, H. (2006). VIP receptors control excitability of suprachiasmatic nuclei

neurones. Pflugers Arch. *452*, 7–15. https://doi.org/10.1007/S00424-005-0003-Z.

41. Cutler, D.J., Haraura, M., Reed, H.E., Shen, S., Sheward, W.J., Morrison, C.F., Marston, H.M., Harmar, A.J., and Piggins, H.D. (2003). The mouse VPAC2 receptor confers suprachiasmatic nuclei cellular rhythmicity and responsiveness to vasoactive intestinal polypeptide in vitro. Eur. J. Neurosci. *17*, 197–204. https://doi.org/10.1046/J.1460-9568.2003.02425.X.

42. Itri, J.N., Michel, S., Vansteensel, M.J., Meijer, J.H., and Colwell, C.S. (2005). Fast delayed rectifier potassium current is required for circadian neural activity. Nat. Neurosci. *8*, 650–656. https://doi.org/10.1038/NN1448.

43. Han, H., Myllykoski, M., Ruskamo, S., Wang, C., and Kursula, P. (2013). Myelin-specific proteins: a structurally diverse group of membrane-interacting molecules. Biofactors *39*, 233–241. https://doi.org/10.1002/BIOF.1076.

44. Kanehisa, M., and Goto, S. (2000). KEGG: kyoto encyclopedia of genes and genomes. Nucleic Acids Res. *28*, 27–30. https://doi.org/10.1093/NAR/28.1.27.

45. Doi, M., Ishida, A., Miyake, A., Sato, M., Komatsu, R., Yamazaki, F., Kimura, I., Tsuchiya, S., Kori, H., Seo, K., et al. (2011). Circadian regulation of intracellular G-protein signalling mediates intercellular synchrony and rhythmicity in the suprachiasmatic nucleus. Nat. Commun. *2*, 327. https://doi.org/10.1038/ncomms1316.

46. Scheer, F.A.J.L., and Shea, S.A. (2014). Human circadian system causes a morning peak in prothrombotic plasminogen activator inhibitor-1 (PAI-1) independent of the sleep/wake cycle. Blood *123*, 590–593. https://doi.org/10.1182/BLOOD-2013-07-517060.

47. Araki, Y., Hong, I., Gamache, T.R., Ju, S., Collado-Torres, L., Shin, J.H., and Huganir, R.L. (2020). Syngap isoforms differentially regulate synaptic plasticity and dendritic development. Elife *9*, e56273. https://doi.org/10.7554/ELIFE.56273.

48. Grand, R.S., Burger, L., Gräwe, C., Michael, A.K., Isbel, L., Hess, D., Hoerner, L., Iesmantavicius, V., Durdu, S., Pregnolato, M., et al. (2021). BANP opens chromatin and activates CpG-island-regulated genes. Nature *596*, 133–137. https://doi.org/10.1038/S41586-021-03689-8.

49. Pichler, I., Schwienbacher, C., Zanon, A., Fuchsberger, C., Serafin, A., Facheris, M.F., Marroni, F., Pattaro, C., Shen, Y., Tellgren-Roth, C., et al. (2013). Fine-mapping of restless legs locus 4 (RLS4) identifies a haplotype over the SPATS2L and KCTD18 genes. J. Mol. Neurosci. *49*, 600–605. https://doi.org/10.1007/S12031-012-9891-5.

50. Clayton, S.A., Daley, K.K., MacDonald, L., Fernandez-Vizarra, E., Bottegoni, G., O'Neil, J.D., Major, T., Griffin, D., Zhuang, Q., Adewoye, A.B., et al. (2021). Inflammation causes remodeling of mitochondrial cytochrome c oxidase mediated by the bifunctional gene C15orf48. Sci. Adv. *7*, eabl5182. https://doi.org/10.1126/SCIADV.ABL5182.

51. Watson, K., and Baar, K. (2014). mTOR and the health benefits of exercise. Semin. Cell Dev. Biol. *36*, 130–139. https://doi.org/10.1016/J.SEMCDB.2014.08.013.

52. Chang, S.W., Yoshihara, T., Tsuzuki, T., Natsume, T., Kakigi, R., Machida, S., and Naito, H. (2022). Circadian rhythms modulate the effect of eccentric exercise on rat soleus muscles. PLoS One *17*, e0264171. https://doi.org/10.1371/JOURNAL.PONE.0264171.

53. Doi, M., Murai, I., Kunisue, S., Setsu, G., Uchio, N., Tanaka, R., Kobayashi, S., Shimatani, H., Hayashi, H., Chao, H.W., et al. (2016). Gpr176 is a Gz-linked orphan G-protein-coupled receptor that sets the pace of circadian behaviour. Nat. Commun. *7*, 10583. https://doi.org/10.1038/NCOMMS10583.

54. Yao, H., Arunachalam, G., Hwang, J.-W., Chung, S., Sundar, I.K., Kinnula, V.L., Crapo, J.D., and Rahman, I. (2010). Extracellular superoxide dismutase protects against pulmonary emphysema by attenuating oxidative fragmentation of ECM. Proc. Natl. Acad. Sci. USA *107*, 15571–15576. https://doi.org/10.1073/pnas.1007625107.

55. Kanno, N., Fujiwara, K., Yoshida, S., Kato, T., and Kato, Y. (2019). Dynamic changes in the localization of neuronatin-positive cells during neurogenesis in the embryonic rat brain. Cells Tissues Organs *207*, 127–137. https://doi.org/10.1159/000504359.

56. Rogers, N., Cheah, P.S., Szarek, E., Banerjee, K., Schwartz, J., and Thomas, P. (2013). Expression of the murine transcription factor SOX3 during embryonic and adult neurogenesis. Gene Expr. Patterns *13*, 240–248. https://doi.org/10.1016/J.GEP.2013.04.004.

57. Yang, M., Gu, Y.Y., Peng, H., Zhao, M., Wang, J., Huang, S.K., Yuan, X.H., Li, J., Sang, J.L., Luo, Q., et al. (2015). NAIF1 inhibits gastric cancer cells migration and invasion via the MAPK pathways. J. Cancer Res. Clin. Oncol. *141*, 1037–1047. https://doi.org/10.1007/S00432-014-1865-2.

58. Zhang, X., Ge, Y.L., Zhang, S.P., Yan, P., and Tian, R.H. (2014). Downregulation of KDR expression induces apoptosis in breast cancer cells. Cell. Mol. Biol. Lett. *19*, 527–541. https://doi.org/10.2478/S11658-014-0210-8.

59. Sutton, G.M., Perez-Tilve, D., Nogueiras, R., Fang, J., Kim, J.K., Cone, R.D., Gimble, J.M., Tschöp, M.H., and Butler, A.A. (2008). The melanocortin-3 receptor is required for entrainment to meal intake. J. Neurosci. *28*, 12946–12955. https://doi.org/10.1523/JNEUROSCI.3615-08.2008.

60. Cheng, M.Y., Bullock, C.M., Li, C., Lee, A.G., Bermak, J.C., Belluzzi, J., Weaver, D.R., Leslie, F.M., and Zhou, Q.Y. (2002). Prokineticin 2 transmits the behavioural circadian rhythm of the suprachiasmatic nucleus. Nature *417*, 405–410. https://doi.org/10.1038/417405A.

61. Dardente, H., Menet, J.S., Challet, E., Tournier, B.B., Pévet, P., and Masson-Pévet, M. (2004). Daily and circadian expression of neuropeptides in the suprachiasmatic nuclei of nocturnal and diurnal rodents. Brain Res. Mol. Brain Res. *124*, 143–151. https://doi.org/10.1016/J.MOLBRAINRES.2004.01.010.

62. Harmar, A.J., Sheward, W.J., Morrison, C.F., Waser, B., Gugger, M., and Reubi, J.C. (2004). Distribution of the VPAC2 receptor in peripheral tissues of the mouse. Endocrinology *145*, 1203–1210. https://doi.org/10.1210/EN.2003-1058.

63. Panda, S., Antoch, M.P., Miller, B.H., Su, A.I., Schook, A.B., Straume, M., Schultz, P.G., Kay, S.A., Takahashi, J.S., and Hogenesch, J.B. (2002). Coordinated transcription of key pathways in the mouse by the circadian clock. Cell *109*, 307–320. https://doi.org/10.1016/S0092-8674(02)00722-5.

64. Hughes, M.E., DiTacchio, L., Hayes, K.R., Vollmers, C., Pulivarthy, S., Baggs, J.E., Panda, S., and Hogenesch, J.B. (2009). Harmonics of circadian gene transcription in mammals. PLoS Genet. *5*, e1000442. https://doi.org/10.1371/JOURNAL.PGEN.1000442.

65. van der Horst, G.T., Muijtjens, M., Kobayashi, K., Takano, R., Kanno, S., Takao, M., de Wit, J., Verkerk, A., Eker, A.P., van Leenen, D., et al. (1999). Mammalian Cry1 and Cry2 are essential for maintenance of circadian rhythms. Nature *398*, 627–630. https://doi.org/10.1038/19323.

66. Okamura, H., Miyake, S., Sumi, Y., Yamaguchi, S., Yasui, A., Muijtjens, M., Hoeijmakers, J.H., and van der Horst, G.T. (1999). Photic induction of mPer1 and mPer2 in cry-deficient mice lacking a biological clock. Science *286*, 2531–2534. https://doi.org/10.1126/SCIENCE.286.5449.2531.

67. Kume, K., Zylka, M.J., Sriram, S., Shearman, L.P., Weaver, D.R., Jin, X., Maywood, E.S., Hastings, M.H., and Reppert, S.M. (1999). mCRY1 and mCRY2 are essential components of the negative limb of the circadian clock feedback loop. Cell *98*, 193–205. https://doi.org/10.1016/S0092-8674(00)81014-4.

68. Harmar, A.J., Arimura, A., Gozes, I., Journot, L., Laburthe, M., Pisegna, J.R., Rawlings, S.R., Robberecht, P., Said, S.I., Sreedharan, S.P., et al. (1998). International union of pharmacology. XVIII. Nomenclature of receptors for vasoactive intestinal peptide and pituitary adenylate cyclase-activating polypeptide. Pharmacol. Rev. *50*, 265–270.

69. Castro-Mondragon, J.A., Riudavets-Puig, R., Rauluseviciute, I., Lemma, R.B., Turchi, L., Blanc-Mathieu, R., Lucas, J., Boddie, P., Khan, A., Manosalva Pérez, N., et al. (2022). JASPAR 2022: the 9th release of the open-access database of transcription factor binding profiles. Nucleic Acids Res. *50*, D165–D173. https://doi.org/10.1093/NAR/GKAB1113.

70. Pembroke, W.G., Babbs, A., Davies, K.E., Ponting, C.P., and Oliver, P.L. (2015).

Temporal transcriptomics suggest that twin-peaking genes reset the clock. Elife *4*, e10518. https://doi.org/10.7554/ELIFE.10518.

71. Maywood, E.S., and Mrosovsky, N. (2001). A molecular explanation of interactions between photic and non-photic circadian clock-resetting stimuli. Brain Res. Gene Expr. Patterns *1*, 27–31. https://doi.org/10.1016/S1567-133X(01)00005-9.

72. Park, J., Zhu, H., O'Sullivan, S., Ogunnaike, B.A., Weaver, D.R., Schwaber, J.S., and Vadigepalli, R. (2016). Single-cell transcriptional analysis reveals novel neuronal phenotypes and interaction networks involved in the central circadian clock. Front. Neurosci. *10*, 481. https://doi.org/10.3389/FNINS.2016.00481.

73. Wen, S., Ma, D., Zhao, M., Xie, L., Wu, Q., Gou, L., Zhu, C., Fan, Y., Wang, H., and Yan, J. (2020). Spatiotemporal single-cell analysis of gene expression in the mouse suprachiasmatic nucleus. Nat. Neurosci. *23*, 456–467. https://doi.org/10.1038/S41593-020-0586-X.

74. Morris, E.L., Patton, A.P., Chesham, J.E., Crisp, A., Adamson, A., and Hastings, M.H. (2021). Single-cell transcriptomics of suprachiasmatic nuclei reveal a Prokineticin-driven circadian network. EMBO J. *40*, e108614. https://doi.org/10.15252/EMBJ.2021108614.

75. Abrahamson, E.E., and Moore, R.Y. (2001). The posterior hypothalamic area: chemoarchitecture and afferent connections. Brain Res. *889*, 1–22. https://doi.org/10.1016/S0006-8993(00)03015-8.

76. Varadarajan, S., Tajiri, M., Jain, R., Holt, R., Ahmed, Q., Lesauter, J., and Silver, R. (2018). Connectome of the suprachiasmatic nucleus: new evidence of the core-shell relationship. eNeuro *5*. ENEURO.0205-18.2018. https://doi.org/10.1523/ENEURO.0205-18.2018.

77. Kalamatianos, T., Kalló, I., and Coen, C.W. (2004). Ageing and the diurnal expression of the mRNAs for vasopressin and for the V1a and V1b vasopressin receptors in the suprachiasmatic nucleus of male rats. J. Neuroendocrinol. *16*, 493–501. https://doi.org/10.1111/J.1365-2826.2004.01196.X.

78. Kalló, I., Kalamatianos, T., Wiltshire, N., Shen, S., Sheward, W.J., Harmar, A.J., and Coen, C.W. (2004). Transgenic approach reveals expression of the VPAC2 receptor in phenotypically defined neurons in the mouse suprachiasmatic nucleus and in its efferent target sites. Eur. J. Neurosci. *19*, 2201–2211. https://doi.org/10.1111/J.0953-816X.2004.03335.X.

79. An, S., Tsai, C., Ronecker, J., Bayly, A., and Herzog, E.D. (2012). Spatiotemporal distribution of vasoactive intestinal polypeptide receptor 2 in mouse suprachiasmatic nucleus. J. Comp. Neurol. *520*, 2730–2741. https://doi.org/10.1002/CNE.23078.

80. Moore, R.Y., Speh, J.C., and Leak, R.K. (2002). Suprachiasmatic nucleus organization. Cell Tissue Res. *309*, 89–98. https://doi.org/10.1007/S00441-002-0575-2.

81. Albers, H.E., Walton, J.C., Gamble, K.L., McNeill, J.K., and Hummer, D.L. (2017). The dynamics of GABA signaling: revelations from the circadian pacemaker in the suprachiasmatic nucleus. Front. Neuroendocrinol. *44*, 35–82. https://doi.org/10.1016/J.YFRNE.2016.11.003.

82. Aton, S.J., Huettner, J.E., Straume, M., and Herzog, E.D. (2006). GABA and Gi/o differentially control circadian rhythms and synchrony in clock neurons. Proc. Natl. Acad. Sci. USA *103*, 19188–19193. https://doi.org/10.1073/PNAS.0607466103.

83. Freeman, G.M., Krock, R.M., Aton, S.J., Thaben, P., and Herzog, E.D. (2013). GABA networks destabilize genetic oscillations in the circadian pacemaker. Neuron *78*, 799–806. https://doi.org/10.1016/J.NEURON.2013.04.003.

84. Ono, D., Honma, K.I., Yanagawa, Y., Yamanaka, A., and Honma, S. (2019). GABA in the suprachiasmatic nucleus refines circadian output rhythms in mice. Commun. Biol. *2*, 232. https://doi.org/10.1038/S42003-019-0483-6.

85. Maejima, T., Tsuno, Y., Miyazaki, S., Tsuneoka, Y., Hasegawa, E., Islam, M.T., Enoki, R., Nakamura, T.J., and Mieda, M. (2021). GABA from vasopressin neurons regulates the time at which suprachiasmatic nucleus molecular clocks enable circadian behavior. Proc. Natl. Acad. Sci. USA *118*. e2010168118. https://doi.org/10.1073/PNAS.2010168118.

86. Greenwood, M., Greenwood, M.P., Paton, J.F.R., and Murphy, D. (2015). Transcription factor CREB3L1 regulates endoplasmic reticulum stress response genes in the osmotically challenged rat hypothalamus. PLoS One *10*, e0124956. https://doi.org/10.1371/JOURNAL.PONE.0124956.

87. Belle, M.D.C., and Diekman, C.O. (2018). Neuronal oscillations on an ultra-slow timescale: daily rhythms in electrical activity and gene expression in the mammalian master circadian clockwork. Eur. J. Neurosci. *48*, 2696–2717. https://doi.org/10.1111/EJN.13856.

88. Brown, T.M., and Piggins, H.D. (2007). Electrophysiology of the suprachiasmatic circadian clock. Prog. Neurobiol. *82*, 229–255. https://doi.org/10.1016/J.PNEUROBIO.2007.05.002.

89. Colwell, C.S., Michel, S., Itri, J., Rodriguez, W., Tam, J., Lelievre, V., Hu, Z., Liu, X., and Waschek, J.A. (2003). Disrupted circadian rhythms in VIP- and PHI-deficient mice. Am. J. Physiol. Regul. Integr. Comp. Physiol. *285*, R939–R949. https://doi.org/10.1152/AJPREGU.00200.2003.

90. Loh, D.H., Dragich, J.M., Kudo, T., Schroeder, A.M., Nakamura, T.J., Waschek, J.A., Block, G.D., and Colwell, C.S. (2011). Effects of vasoactive intestinal peptide genotype on circadian gene expression in the suprachiasmatic nucleus and peripheral organs. J. Biol. Rhythms *26*, 200–209. https://doi.org/10.1177/0748730411401740.

91. Yamaguchi, S., Isejima, H., Matsuo, T., Okura, R., Yagita, K., Kobayashi, M., and Okamura, H. (2003). Synchronization of cellular clocks in the suprachiasmatic nucleus. Science *302*, 1408–1412. https://doi.org/10.1126/SCIENCE.1089287.

92. Rusnak, M., Tóth, Z.E., House, S.B., and Gainer, H. (2007). Depolarization and neurotransmitter regulation of vasopressin gene expression in the rat suprachiasmatic nucleus in vitro. J. Neurosci. *27*, 141–151. https://doi.org/10.1523/JNEUROSCI.3739-06.2007.

93. Feng, D., Liu, T., Sun, Z., Bugge, A., Mullican, S.E., Alenghat, T., Liu, X.S., and Lazar, M.A. (2011). A circadian rhythm orchestrated by histone deacetylase 3 controls hepatic lipid metabolism. Science *331*, 1315–1319. https://doi.org/10.1126/SCIENCE.1198125.

94. Azzi, A., Dallmann, R., Casserly, A., Rehrauer, H., Patrignani, A., Maier, B., Kramer, A., and Brown, S.A. (2014). Circadian behavior is light-reprogrammed by plastic DNA methylation. Nat. Neurosci. *17*, 377–382. https://doi.org/10.1038/NN.3651.

95. Zhang, J., Kalkum, M., Chait, B.T., and Roeder, R.G. (2002). The N-CoR-HDAC3 nuclear receptor corepressor complex inhibits the JNK pathway through the integral subunit GPS2. Mol. Cell *9*, 611–623. https://doi.org/10.1016/S1097-2765(02)00468-9.

96. Alenghat, T., Meyers, K., Mullican, S.E., Leitner, K., Adeniji-Adele, A., Avila, J., Bućan, M., Ahima, R.S., Kaestner, K.H., and Lazar, M.A. (2008). Nuclear receptor corepressor and histone deacetylase 3 govern circadian metabolic physiology. Nature *456*, 997–1000. https://doi.org/10.1038/NATURE07541.

97. Kokura, K., Kaul, S.C., Wadhwa, R., Nomura, T., Khan, M.M., Shinagawa, T., Yasukawa, T., Colmenares, C., and Ishii, S. (2001). The Ski protein family is required for MeCP2-mediated transcriptional repression. J. Biol. Chem. *276*, 34115–34121. https://doi.org/10.1074/JBC.M105747200.

98. Aninye, I.O., Matsumoto, S., Sidhaye, A.R., and Wondisford, F.E. (2014). Circadian regulation of Tshb gene expression by Rev-Erbα (NR1D1) and nuclear corepressor 1 (NCOR1). J. Biol. Chem. *289*, 17070–17077. https://doi.org/10.1074/JBC.M114.569723.

99. Kim, Y.H., Marhon, S.A., Zhang, Y., Steger, D.J., Won, K.J., and Lazar, M.A. (2018). Rev-erbα dynamically modulates chromatin looping to control circadian gene transcription. Science *359*, 1274–1277. https://doi.org/10.1126/SCIENCE.AAO6891.

100. Yamaguchi, Y., Murai, I., Takeda, M., Doi, S., Seta, T., Hanada, R., Kangawa, K., Okamura, H., Miyake, T., and Doi, M. (2022). Nmu/Nms/Gpr176 triple-deficient mice show enhanced light-resetting of circadian

locomotor activity. Biol. Pharm. Bull. *45*, 1172–1179. https://doi.org/10.1248/BPB.B22-00260.

101. Hamnett, R., Chesham, J.E., Maywood, E.S., and Hastings, M.H. (2021). The cell-autonomous clock of VIP receptor VPAC2 cells regulates period and coherence of circadian behavior. J. Neurosci. *41*, 502–512. https://doi.org/10.1523/JNEUROSCI.2015-20.2020.

102. Abe, M., Herzog, E.D., Yamazaki, S., Straume, M., Tei, H., Sakaki, Y., Menaker, M., and Block, G.D. (2002). Circadian rhythms in isolated brain regions. J. Neurosci. *22*, 350–356. https://doi.org/10.1523/JNEUROSCI.22-01-00350.2002.

103. Granados-Fuentes, D., Saxena, M.T., Prolo, L.M., Aton, S.J., and Herzog, E.D. (2004). Olfactory bulb neurons express functional, entrainable circadian rhythms. Eur. J. Neurosci. *19*, 898–906. https://doi.org/10.1111/J.0953-816X.2004.03117.X.

104. Guilding, C., Hughes, A.T.L., Brown, T.M., Namvar, S., and Piggins, H.D. (2009). A riot of rhythms: neuronal and glial circadian oscillators in the mediobasal hypothalamus. Mol. Brain *2*, 28. https://doi.org/10.1186/1756-6606-2-28.

105. Harbour, V.L., Weigl, Y., Robinson, B., and Amir, S. (2013). Comprehensive mapping of regional expression of the clock protein PERIOD2 in rat forebrain across the 24-h day. PLoS One *8*, e76391. https://doi.org/10.1371/JOURNAL.PONE.0076391.

106. Northeast, R.C., Chrobok, L., Hughes, A.T.L., Petit, C., and Piggins, H.D. (2020). Keeping time in the lamina terminalis: novel oscillator properties of forebrain sensory circumventricular organs. FASEB J. *34*, 974–987. https://doi.org/10.1096/FJ.201901111R.

107. Guilding, C., and Piggins, H.D. (2007). Challenging the omnipotence of the suprachiasmatic timekeeper: are circadian oscillators present throughout the mammalian brain? Eur. J. Neurosci. *25*, 3195–3216. https://doi.org/10.1111/J.1460-9568.2007.05581.X.

108. Mendoza, J., and Challet, E. (2009). Brain clocks: from the suprachiasmatic nuclei to a cerebral network. Neuroscientist *15*, 477–488. https://doi.org/10.1177/1073858408327808.

109. Sheward, W.J., Maywood, E.S., French, K.L., Horn, J.M., Hastings, M.H., Seckl, J.R., Holmes, M.C., and Harmar, A.J. (2007). Entrainment to feeding but not to light: circadian phenotype of VPAC2 receptor-null mice. J. Neurosci. *27*, 4351–4358. https://doi.org/10.1523/JNEUROSCI.4843-06.2007.

110. Georg, B., Fahrenkrug, J., Jørgensen, H.L., and Hannibal, J. (2021). The circadian clock is sustained in the thyroid gland of VIP receptor 2 deficient mice. Front. Endocrinol. *12*, 1100. https://doi.org/10.3389/FENDO.2021.737581/BIBTEX.

111. Stephan, F.K. (2002). The "other" circadian system: food as a Zeitgeber. J. Biol. Rhythms *17*, 284–292. https://doi.org/10.1177/074873040201700402.

112. Stephan, F.K., Swann, J.M., and Sisk, C.L. (1979). Anticipation of 24-hr feeding schedules in rats with lesions of the suprachiasmatic nucleus. Behav. Neural. Biol. *25*, 346–363. https://doi.org/10.1016/S0163-1047(79)90415-1.

113. Honma, S., Honma, K., and Hiroshige, T. (1991). Methamphetamine effects on rat circadian clock depend on actograph. Physiol. Behav. *49*, 787–795. https://doi.org/10.1016/0031-9384(91)90319-J.

114. Mistlberger, R.E. (1994). Circadian food-anticipatory activity: formal models and physiological mechanisms. Neurosci. Biobehav. Rev. *18*, 171–195. https://doi.org/10.1016/0149-7634(94)90023-X.

115. Saul, M.C., Majdak, P., Perez, S., Reilly, M., Garland, T., and Rhodes, J.S. (2017). High motivation for exercise is associated with altered chromatin regulators of monoamine receptor gene expression in the striatum of selectively bred mice. Genes Brain Behav. *16*, 328–341. https://doi.org/10.1111/GBB.12347.

116. Lananna, B.v., and Musiek, E.S. (2020). The wrinkling of time: aging, inflammation, oxidative stress, and the circadian clock in neurodegeneration. Neurobiol. Dis. *139*, 104832. https://doi.org/10.1016/J.NBD.2020.104832.

117. Leng, Y., Musiek, E.S., Hu, K., Cappuccio, F.P., and Yaffe, K. (2019). Association between circadian rhythms and neurodegenerative diseases. Lancet Neurol. *18*, 307–318. https://doi.org/10.1016/S1474-4422(18)30461-7.

118. Bolger, A.M., Lohse, M., and Usadel, B. (2014). Trimmomatic: a flexible trimmer for Illumina sequence data. Bioinformatics *30*, 2114–2120. https://doi.org/10.1093/BIOINFORMATICS/BTU170.

119. Kim, D., Langmead, B., and Salzberg, S.L. (2015). HISAT: a fast spliced aligner with low memory requirements. Nat. Methods *12*, 357–360. https://doi.org/10.1038/NMETH.3317.

120. Pertea, M., Kim, D., Pertea, G.M., Leek, J.T., and Salzberg, S.L. (2016). Transcript-level expression analysis of RNA-seq experiments with HISAT, StringTie and Ballgown. Nat. Protoc. *11*, 1650–1667. https://doi.org/10.1038/nprot.2016.095.

121. Pertea, M., Pertea, G.M., Antonescu, C.M., Chang, T.C., Mendell, J.T., and Salzberg, S.L. (2015). StringTie enables improved reconstruction of a transcriptome from RNA-seq reads. Nat. Biotechnol. *33*, 290–295. https://doi.org/10.1038/nbt.3122.

122. Frankish, A., Diekhans, M., Ferreira, A.M., Johnson, R., Jungreis, I., Loveland, J., Mudge, J.M., Sisu, C., Wright, J., Armstrong, J., et al. (2019). GENCODE reference annotation for the human and mouse genomes. Nucleic Acids Res. *47*, D766–D773. https://doi.org/10.1093/nar/gky955.

123. Wu, T., Hu, E., Xu, S., Chen, M., Guo, P., Dai, Z., Feng, T., Zhou, L., Tang, W., Zhan, L., et al. (2021). clusterProfiler 4.0: a universal enrichment tool for interpreting omics data. Innovation *2*, 100141. https://doi.org/10.1016/J.XINN.2021.100141.

124. Alexa, A., and Rahnenfuhrer, J. (2016). topGO: Enrichment analysis for Gene Ontolgy. R package version 2.28.0 (Cranio).

125. Love, M.I., Huber, W., and Anders, S. (2014). Moderated estimation of fold change and dispersion for RNA-seq data with DESeq2. Genome Biol. *15*, 550. https://doi.org/10.1186/S13059-014-0550-8.

126. Wegner, S., Belle, M.D.C., Hughes, A.T.L., Diekman, C.O., and Piggins, H.D. (2017). Delayed cryptochrome degradation asymmetrically alters the daily rhythm in suprachiasmatic clock neuron excitability. J. Neurosci. *37*, 7824–7836. https://doi.org/10.1523/JNEUROSCI.0691-17.2017.

127. Livak, K.J., and Schmittgen, T.D. (2001). Analysis of relative gene expression data using real-time quantitative PCR and the 2(-Delta Delta C(T)) Method. Methods *25*, 402–408. https://doi.org/10.1006/METH.2001.1262.

128. Afgan, E., Baker, D., Batut, B., van den Beek, M., Bouvier, D., Cech, M., Chilton, J., Clements, D., Coraor, N., Grüning, B.A., et al. (2018). The Galaxy platform for accessible, reproducible and collaborative biomedical analyses: 2018 update. Nucleic Acids Res. *46*, W537–W544. https://doi.org/10.1093/NAR/GKY379.

129. Brown, L.A., Williams, J., Taylor, L., Thomson, R.J., Nolan, P.M., Foster, R.G., and Peirson, S.N. (2017). Meta-analysis of transcriptomic datasets identifies genes enriched in the mammalian circadian pacemaker. Nucleic Acids Res. *45*, 9860–9873. https://doi.org/10.1093/NAR/GKX714.

STAR★METHODS

KEY RESOURCES TABLE

REAGENT or RESOURCE	SOURCE	IDENTIFIER
Critical commercial assays		
ReliaPrep RNA tissue Miniprep System	Promega, USA	Cat# Z6112
High-Capacity RNA-to-cDNA Kit	Applied Biosystems, USA	Cat# 10704217
TaqMan™ Gene Expression assay	Applied Biosystems, USA	Cat# 4331182
RNA 6000 Pico Kit	Agilent Technologies, USA	Cat# 5067-1513
Sense Total RNA-Seq Library Prep Kit	Lexogen, USA	Cat# 001.24
Experimental models: Organisms/strains		
Mouse: C57BL/6JRccHsd	Envigo (Harlan), Blackthorn, UK	https://www.envigo.com/model/c57bl-6jrcchsd
Mouse: Vipr2$^{-/-}$ (C57BL/6J background)	Harmar et al.[12]	N/A
Mouse: Cry1$^{-/-}$/Cry2$^{-/-}$ (C57BL/6 background)	van der Horst et al.[65]	N/A
Software and algorithms		
Trimmomatic	Bolger et al.[118]	http://www.usadellab.org/cms/?page=trimmomatic
HISAT2 aligner	Kim et al.[119]	http://daehwankimlab.github.io/hisat2/
Stringtie	Pertea et al.[120,121]	https://ccb.jhu.edu/software/stringtie/
Clocklab	Actimetrics	https://actimetrics.com/products/clocklab/
GENCODE	Frankish et al.[122]	https://www.gencodegenes.org/
Bioconductor 3.14, R (R Core Team (2020). R: A language and environment for statistical computing.	R Foundation for Statistical Computing, Vienna, Austria	https://cran.r-project.org/
Inkscape	The Inkscape Team	https://inkscape.org/
Powerpoint ver. 2110	Microsoft, USA	N/A
Excel ver. 2110	Microsoft, USA	N/A
ClusterProfiler	Wu et al.[123]	https://bioconductor.org/packages/release/bioc/html/clusterProfiler.html
TopGO	Alexa et al.[124]	https://bioconductor.org/packages/release/bioc/html/topGO.html
DeSeq2	Love et al.[125]	https://bioconductor.org/packages/release/bioc/html/DESeq2.html
Quantification and data analysis	N/A	N/A
Prism version 9	Graphpad, San Diego, CA	https://www.graphpad.com/scientific-software/prism/
Other		
PhenoMaster acquisition system	TSE Systems, Bad Homburg, Germany	https://www.tse-systems.com/service/phenomaster/
Chronobiology Kit	(Stanford Software Systems, Naalehu, HI	https://www.query.com/chronokit/
Deposited data	This paper	GEO: GSE207992

RESOURCE AVAILABILITY

Lead contact

Further information and requests for resources, reagents and token to access the GEO database should be directed to and will be fulfilled by the lead contact, Prof. Hugh Piggins (hugh.piggins@bristol.ac.uk).

Materials availability

This study did not generate new unique reagents.

Data and code availability

RNA-seq data have been deposited at GEO: GSE207992, and are publicly available from the date of publication.

EXPERIMENTAL MODEL AND SUBJECT DETAILS

All procedures were carried out under the UK Animals (Scientific Procedures) Act (1986) and approved by the University of Manchester Review Ethics Panel. Most experiments were conducted on adult male mice (8-20 weeks of age) of two genotypes: C57BL/6 (wild-type, *Vipr2*$^{+/+}$; Envigo (Harlan), Blackthorn, UK) and transgenic mice lacking the $VPAC_2$ receptor, *Vipr2*$^{-/-}$ (C57BL/6 background; initial breeding stock of *Vipr2*$^{-/-}$ donated by A. Harmar, University of Edinburgh). A cohort of adult male *Cry1*$^{-/-}$*Cry2*$^{-/-}$ mice which lack a functional molecular clock were also used. These animals were derived from initial *Cry1*$^{+/-}$*Cry2*$^{+/-}$ breeding stock donated by G.T. van der Horst, Erasmus University, Rotterdam, Netherlands.[65] Mice were bred and maintained at 20–22 C and ~40% humidity, with *ad libitum* access to food and water prior to and throughout experiments. Breeding rooms were maintained on a 12-h:12-h LD (LD 12:12) cycle. The number of animals per experimental condition is detailed in the figure captions.

METHOD DETAILS

Animals used in these studies were singly housed in running-wheel equipped cages, using protocols established in our laboratory.[21,22,126] For most mice, feeding and drinking were also monitored and recorded using a PhenoMaster acquisition system (TSE Systems, Bad Homburg, Germany). The Phenomaster system can be programmed to control if, when, and for how long a running-wheel can be rotated by a mouse[21] and here it was used to provide a scheduled-voluntary exercise (SVE) regimen. In addition, animals free to utilize the running wheel at any time (non-scheduled exercise or nSVE condition) were also monitored in the Phenomaster system. A further cohort of animals were recorded using the Chronobiology kit (Stanford Software Systems, Naalehu, HI) as previously described.[21,126] This system was configured to record wheel-running and drinking activities.

At the start of behavioral screening, mice were placed for 14 days in LD12:12 and then the lights were turned off and the animals maintained in constant dark (DD) for the remainder of the experiment. In DD, mice were either allowed to free-run for the duration of the experiment (nSVE cohort) or were included in a SVE cohort. For this SVE cohort, animals free ran for 14 days and then their exercise in the running-wheel was restricted for 6h every 24h, at the same time each day. Entrainment to SVE was defined as when the onset of drinking activity showed ~24h periodicity for 6-7 successive days. *Vipr2*$^{-/-}$ animals rapidly respond to SVE and show entrainment within 12 days[21], whereas *Vipr2*$^{+/+}$, mice took >35days. Mice that did not entrain to SVE were not used in subsequent gene expression assessment and similarly, *Vipr2*$^{-/-}$ mice that were arrhythmic or very weakly rhythmic in the nSVE condition were also excluded (approximately 46% of *Vipr2*$^{-/-}$ mice were considered rhythmic, which enabled determination of their CT necessary for accurate determination of the timing of tissue collection). Figure 1 depicts the experimental design.

The two genotypes of mice are known to differ in the phase of their intrinsic circadian cycle that aligns with the opportunity to exercise in the running-wheel.[21,22] For *Vipr2*$^{-/-}$ animals that entrain to SVE, the onset of their circadian rhythm in drinking (CT12) is coincident with the time that the running wheel is available for exercise (ZT12), while for *Vipr2*$^{+/+}$ mice that entrain to SVE, the beginning of their intrinsic drinking rhythm (CT12) occurs ~8h in advance of the opportunity to the exercise in the wheel (ZT12). Consequently, SVE ZT12 for *Vipr2*$^{+/+}$ animals corresponds to their CT20, whereas for *Vipr2*$^{-/-}$ mice, SVE ZT12 is equivalent to CT12.

Once entrained, animals in the SVE cohort whose tissue was to be used in the RNA-seq study, were culled 2h after the time at which the wheel became available to exercise in (ZT14 or CT14 for *Vipr2*$^{-/-}$ mice and ZT14/CT22 for *Vipr2*$^{+/+}$ animals). *Vipr2*$^{-/-}$ and *Vipr2*$^{+/+}$ mice in the SVE condition whose tissues were to be used in the qRT-PCR study were culled at ZT14 (corresponding to CT14 for *Vipr2*$^{-/-}$ animals and CT22 for *Vipr2*$^{+/+}$ animals; see Figure 1 legend for details) with an additional group of *Vipr2*$^{+/+}$ animals sampled at CT14. Animals in the nSVE cohort were culled at one of two timepoints for qRT-PCR (CT0 or CT14) and

one timepoint for RNA-seq (CT14) (see caption of Figure 1). For qRT-PCR, the brain, lungs, and liver were rapidly dissected and flash frozen on dry ice. For RNA-seq, the brain was removed, flash frozen on dry ice, and stored at -80C. Brain sections of 20 μm thickness were cut using a cryostat (Leica CM3050 S) onto PEN-membrane slides (Leica Biosystems, Germany) and then stored at -80°C. Slides were then defrosted and to aid in identifying the SCN and its anatomical boundaries, sections were stained with 1% cresyl violet (Merck) in 70% ethanol. The SCN was identified and extracted on a laser-capture microscope (LCM) system (Leica DM6000 B) and stored in lysis buffer (Promega) prior to RNA extraction. A cohort of *Cry1*$^{-/-}$*Cry2*$^{-/-}$ animals (n=8) were singly housed and their drinking and wheel-running activity recorded using the Chronobiology Kit. These mice were subject to similar protocols as described above and were maintained on the timed exercise protocol for 22 days and then left to freely exercise for another 11 days in constant darkness. Parameters of their wheel-running were assessed as described above. The activity of these *Cry1*$^{-/-}$*Cry2*$^{-/-}$ animals was compared to previously published data from *Vipr2*$^{-/-}$ mice whose activity had been recorded using the Chronobiology Kit and who had been exposed to a similar SVE protocol.[22]

Quantitative RT-PCR

After extracting RNA using the ReliaPrep RNA tissue Miniprep System (Promega, USA) (liver: 600-1700 ng/μl, lung: 90-225 ng/μl of RNA per sample), cDNA was obtained with the High-Capacity RNA-to-cDNA Kit and qRT-PCR was performed using TaqMan Gene Expression assays (both from Applied Biosystems, USA), on a StepOnePlus Real-Time PCR system (Life Technologies, USA). The relative quantification for each gene was obtained with the ΔΔCt method.[127] *Tbp* was used as the housekeeping gene, and the mean values of *Vipr2*$^{+/+}$ or *Vipr2*$^{-/-}$ nSVE CT14 were used to normalize within genotype comparisons, while normalization to *Vipr2*$^{+/+}$ nSVE CT14 was used for intergenotype comparisons. The following primers were used: Mm01271704_m1 (*Avp*), Mm00500226_m1 (*Bmal1*), Mm00445553_m1 (*Cxcl12*), Mm00725701_s1 (*Glul*), Mm01267381_g1 (*Gys2*), Mm00434876_s1 (*Mc3r*), Mm00520708_m1 (*Nr1d1*), Mm00440701_m1 (*Pdgfra*), Mm00478099_m1 (*Per2*), Mm00440939_m1 (*Pparα*), Mm07298039_m1 (*Prok2*), Mm00803538_m1 (*Tgfbr3*), all TaqMan Gene Expression assay primers (Life Technologies Ltd, UK).

RNA-seq

Samples of SCN from four experimental groups were used to assess gene expression by bulk RNA-seq analysis and included: *Vipr2*$^{+/+}$ nSVE CT14 (n=4), *Vipr2*$^{+/+}$ SVE ZT14/CT24 (n=4), *Vipr2*$^{-/-}$ nSVE CT14 (n=3), and *Vipr2*$^{-/-}$ SVE ZT14/CT14 (n=3). RNA extraction was carried out with ReliaPrep Kit (Promega, UK), checked with RNA 6000 Pico Kit (Agilent Technologies, USA), and amplified with Sense Total RNA-Seq Library Prep Kit (Lexogen, USA). RNA sequencing (4.2-6.6 ng/μl of RNA per sample) was done by paired-end sequencing on an Illumina HiSeq 4000 NGS platform (Genomic Technologies Core Facility, University of Manchester, UK). Raw reads were uploaded to the Galaxy server[128] at the University of Manchester (https://centaurus.itservices.manchester.ac.uk/). Reads were trimmed with Trimmomatic,[118] aligned to the mouse genome (Version GRCm38) using HISAT2 aligner,[119] and counts calculated using Stringtie[120,121] and annotated based on GENCODE.[122] Differential gene expression was analysed using DeSeq2,[125] which applied by default an independent filtering based on the mean of normalized counts, as well as a Cook's distance threshold to remove outliers. The total number of genes passing this filtering/thresholding in each pairwise analysis was: 9524 in *Vipr2*$^{+/+}$ SVE vs *Vipr2*$^{+/+}$ nSVE, 15735 in *Vipr2*$^{-/-}$ SVE vs *Vipr2*$^{-/-}$ nSVE, 10488 in *Vipr2*$^{+/+}$ SVE vs *Vipr2*$^{-/-}$ SVE, 15269 in *Vipr2*$^{+/+}$ nSVE vs *Vipr2*$^{-/-}$ nSVE, and 11931 in *Vipr2*$^{+/+}$ nSVE vs *Vipr2*$^{-/-}$ SVE.

After obtaining the differentially expressed genes, the p-value was corrected with the Benjamini Hochberg method to obtain the False Discovery Rate. The data can be accessed at GEO: GSE207992 (https://www.ncbi.nlm.nih.gov/geo/query/).

Assessment of 20 genes identified as being enriched in the mouse SCN in a transcriptome meta-analysis[129] showed all samples expressed 19 of these genes (Figure S6). One gene *RP24-361E14.1*, was not detected in the samples as it could not be located in the Ensembl database. This suggests that our protocols successfully targeted and extracted genetic material from the SCN that are consistent with other investigations.

QUANTIFICATION AND STATISTICAL ANALYSIS

Actograms were constructed and analyzed using the Chi-square periodogram function in ClockLab (Actimetrics). Analysis of RNA-seq data was done in R (Bioconductor 3.14, R (R Core Team (2020). R: A language

and environment for statistical computing. R Foundation for Statistical Computing, Vienna, Austria). Gene enrichment was evaluated with the R packages ClusterProfiler (Kyoto Encyclopedia of Genes and Genomes or KEGG),[123] and TopGO (Gene Ontology, specifically Biological Process).[124] Statistical analysis was performed in R and Prism (ver. 9, Graphpad, San Diego, CA) or Microsoft Excel (Excel ver. 2110). Graphs were constructed using Prism and composed in Microsoft Powerpoint (Powerpoint ver. 2110). Individual statistical tests, significances and sample sizes are reported in the appropriate figure legends. Unless stated otherwise, data are plotted as mean $\pm$ standard error of mean (SEM), with individual data points overlaid. Data for all measurements are available upon reasonable request.